MSA

October University for Modern Science & Arts
Faculty of Engineering
Department of Mechatronics System Engineering

Design and Implementation of an Automated Channel-Fed Drug Dispensing System

A Graduation Project
Submitted in Partial Fulfillment of B.Sc. Degree
Requirements in Mechatronics System Engineering
(Part II)

Prepared By

Ahmed Khalid Ramadan Selem	191727
Ganna Hassan Helmi Hassan	193463

Supervised By

Supervisor 1 Dr. Tarek Mohamed Ghoniemy
Supervisor 2 Dr. Mohamed Ali Abdelnaby

Spring 2023

Abstract

Pharmacy Drug Dispensing System is an advanced system with new technologies that ease human life. The system does not only facilitate human life but also serves critical medical situations; as it responds and acts faster than pharmacists. The system with just a few orders can take and bring the desired medicine ordered without any human intervention or errors.

In the last few years, as the number of patients has been increasing, the demand on medicines is increasing too. In hospitals with a numerous number of patients a pharmacist cannot withstand this number and meets all their requirements in a short time. Therefore, it will cause a lot of errors sometimes wrong medicines that may influence human life. Thus, new technologies must be involved to reduce the error in such a critical field. The need for the drug dispensing system is increasing now to prevent errors and save time.

The project is consisted of a robot mounted on a shelf to dispense drugs. The robot moves in x and y directions to reach each drug location. The drugs are to be stored manually and update the database with each new medicine added to be known by the robot. With the aid of graphical user interface, the customer can order their desired medicines, so the robot goes to their exact locations and fed them to the slider to check if the medicine is correct and transfer it to the customer.

Keywords: Pharmacy, Drug, Medicine, Dispensing.

Table of Contents

List of Figures

List of Tables

List of Abbreviations

AR	Automated Storage	8
AVG	Auto-Guied Vehicle	6
BSD	Ball Screw Drive	22
FIFO	First In First Out	8
LDD	Linear Direct Drive	22
OCR	Optical Character Recognition	27
RPD	Rack and Pinion Drive	22
RRT	Rapidly-exploring Random Tree	3
RS	Retrieval System	8
STD	Standard Deviation	56

Chapter I
Introduction

1.1 Background of the Study

Nowadays with the increase in the human population, the demand for medicines is increasing as well. The traditional way to get a medicine by a pharmacist takes a lot of time, from knowing the order and deliver it to a patient. On the other hand, robots are nowadays widely used in many aspects to improve efficiency and avoid time wasting. From this point of view the idea of the automated drug dispensing robot has come, a robot that can dispense medicines in less time with higher precision on repetitive than a pharmacist. The robot has a lot of ways to be installed in, such as the chaotic storage that usually uses a robotic arm, the channel-fed which usually uses a cartesian mechanism and the gravity shelf that does not need any robot just a conveyor belt to direct the medicines through it to the pickup point (Obayda *et al*, 2017). All these types serve the same objective, which is drug dispensing but each of them has its own advantages and constraints that must be taken into consideration to apply the system. Such a system can know the order with the user interface program and the position of each medicine is to be known from a database, the robot has only the job of going to the position of the medicine, pick it, then dispense it to the customer.

Figure1.1 Real Project of An Automated Cartesian Straight Shelf drug dispenser (Kent *et al*, 2021)

1.2 Problem Definition

Increasing in population all over the world increases the number of patients relatively and the demand for medicines as well. A pharmacist cannot withstand the continuous demand on pharmacies without fatigue or time wasting. Sometimes the orders must be very fast

so that a pharmacist cannot attend and may result in errors in picking the wrong medicine that may lead to health issues. A robot that can take the pharmacist role is a need in these situations as it does not need break time and it is very fast with high accuracy preventing human error.

1.3 Project Aim and Objectives

The aim of the project is to design and implement an automated channel-fed drug dispensing system to help in making the process of drug dispensing easier, faster, and more precise. The objectives of our project are stated in the below points.

- To conduct a literature survey on automated channel-fed drug dispensing system.
- To select design and components based on literature survey.
- To design a cartesian robot for 2D motion.
- To design a suitable shelf that can serve the operation.
- To develop a searching algorithm to make the process of dispensing faster.
- To improve the capacity efficiency of such a system using the proposed shelf.
- To improve the safety of the dispensing process.
- To analyze the system components.
- To model and simulate the system using MATLAB.
- To implement the hardware system.
- To test the system functionality.
- To publish a paper on such a new field.

1.4 Proposed Solution

A proposed solution is to integrate the gravity shelf mechanism with the cartesian robot to improve the speed of dispensing, reduce the foot-print of such a system to improve the storing capacity, and to make the implementation of such a system easier.

1.5 Report Organization

There is 5 chapters in the report, the first chapter introduces the background of the study, and the aims of the project, second chapter is the design of the system, while the third and fourth chapters are discusses the control methodology and the analysis of the results. Last chapter states the future work to be done and the conclusions.

Chapter II
System Design

2.1 Conceptual Design

The project design was chosen to meet the project's requirements and objectives. The mechanical structure was made to increase floor capacity efficiency. The dispensing method was chosen to speed up the dispensing process. This chapter will cover more system design criteria.

2.1.1 Replenishment Process

The shelves should initially be stocked with medications in order to get the system up and running. The pharmacist performs the replenishment process. The medications are fed from the frame's back; each medication has a specific shelf. The pharmacist then updates the database with the new medication's name, shelf number, quantity, etc. The robot is now prepared to dispense.

2.1.2 Dispensing Process

The dispensing procedure begins when a medicine is requested. The pharmacist will order the medications from the screen by typing in the name of the medication or choosing it from a list. After confirming the order, a robot will go to each medication's location and collect it from the shelf. Once all necessary medications have been collected (ideally all at once), the robot will conduct a safety check to ensure that the medications are indeed the necessary ones before dispensing them to the customer via one of the delivery channels.

2.1.3 Internal Process

The internal method outlines what the robot undertakes to complete the task safely and quickly. The robot will first check the database for the requested medicines to see if they are already in stock (the pharmacist will be informed of any unavailable medications by name), then it will specify the location of each requested medication, figure out the fastest way to collect them all, double-check the medication's name to ensure that no incorrect medications are being given out, and finally deliver the requested medications to the customer.

2.1.4 Design Iterations

The design has an important part which is the X-axis. The design of the X-axis is very important as it is the main axis that will hold all the system moving components, so it must be light in weight and have some kind of rigidity. There were many proposed designs for the X-axis, but they were eliminated, due to their high cost, low efficiency, or less rigidity. Finally, there were 2 approaches for the X-axis, one-axis approach, and the two-axis approach, these two approaches are similar in components and have the main motion idea, so to choose the best one a dynamic analysis had to be done first, below figure shows the two approaches.

(a) (b)

Figure2.1 Proposed designs (a) one axis approach, (b) Two axis approach

To validate the design as declared before, a dynamic analysis was applied to obtain the robot speed, position, the different stresses acting on the shaft, and the deformation of the shaft. From these observations it can be decided which approaches to be manufactured, as the output graphs represent the system behavior.

2.1.5 Design Validation

Dynamic analysis is important to verify the system design, as the dynamic analysis is made using Adams Multibody Dynamic Simulator to visualize the motion of the body under all forces that are exerted on it. The dynamic simulation is made on the main part that is responsible for moving the robot's body. The shaft is the part that is responsible for transmitting the motion from the motor to the robot using RPD, the shaft is subjected to many forces as the 6 friction forces from the bearings, normal, and tangential force from the 2 pinions, and the torque from the motor. All these forces make the shaft subjected to failure from high stress or make the motion of the shaft not as expected to be so a dynamic simulation is needed to verify the functionality of the shaft. The first proposed design was to transmit the motion from the motor to the center of mass of the shaft (one axis), this result in high stresses on the shaft, high moment from the friction force; thus, result in deforming the shaft while working until it fails.

One Axis Transmission Approach

At the beginning the shaft was proposed to transfer the motion to the robot using only one pinion that is placed in the middle of the shaft, this design results in high stresses on the shaft as shown in the following figure.

VON MISES Hot Spots for connecting_rod_flex Date= 2023-04-09 23:49:27						
Model= .First		Analysis= Last_Run		Time = 0 to 1 sec		
Top 10 Hot Spots			Abs	Radius= 0 mm		
Hot Spot	Stress	Node	Time	Location wrt LPRF (mm)		
#	(newton/mm**2)	id	(sec)	X	Y	Z
1	34.9431	623	1	321.909	514.532	-287.419
2	32.2872	628	0.99	321.909	478.957	-287.419
3	31.9838	625	1	321.91	499.612	-287.419
4	31.0643	560	1	327.342	514.576	-287.599
5	30.9167	617	1	321.909	558.613	-287.419
6	30.3565	923	0.99	327.776	499.612	-274.488
7	29.7466	630	1	321.909	464.662	-287.419
8	29.3904	618	1	321.91	549.479	-287.419
9	29.1822	931	0.99	327.776	440.609	-274.488
10	29.0626	913	0.95	327.776	570.133	-274.488

Figure2.2 The most 10 nodes in the shaft that are subjected to stress.

As the figure shows the stresses that are exerted on the shaft, they are very high. These stresses lead the shaft to fail the operation of traveling along the axis, although failed to reach its desired speed.

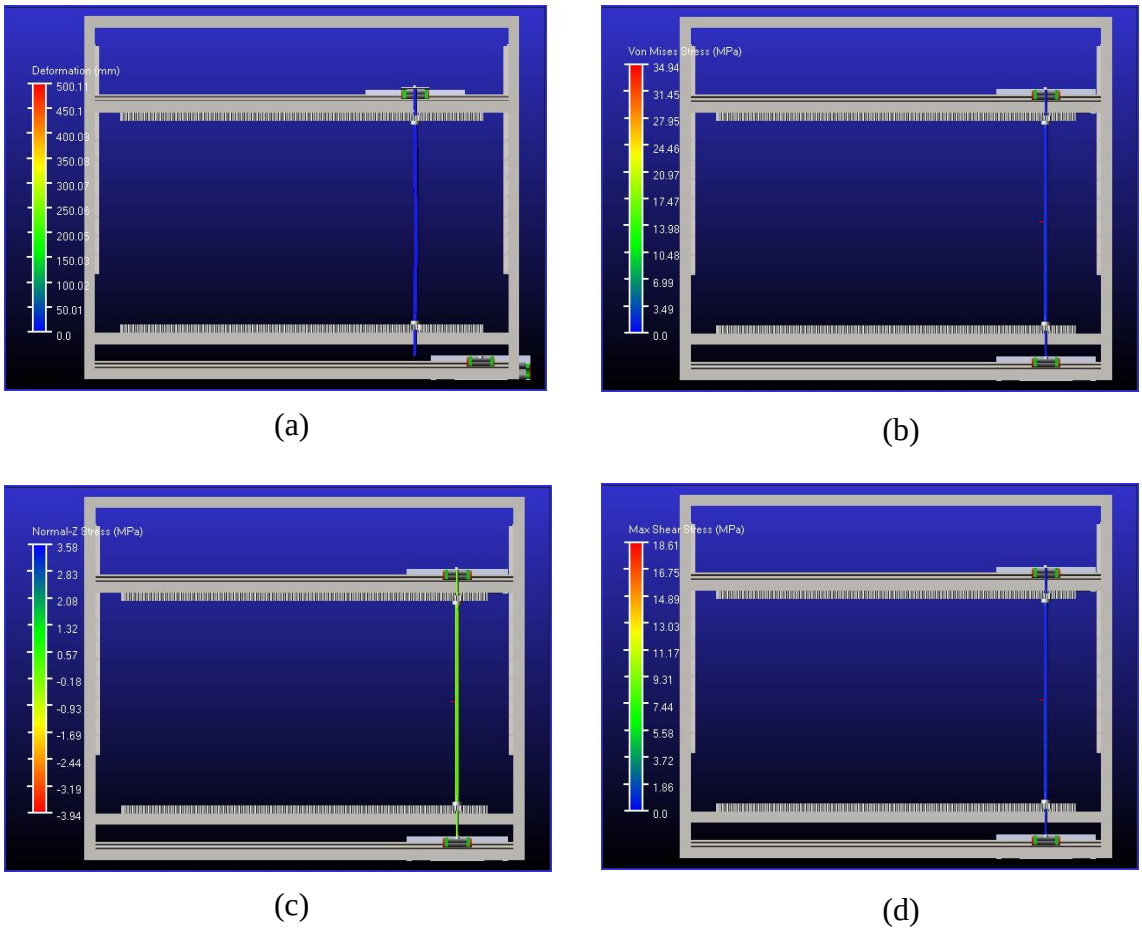

Figure2.3 (a) Deformation, (b) Von-Mises Stress, (c) Shear stress in z direction, and (d) Max shear stress

Figure (2.3) shows the different stresses that act on the shaft. High stress causes the shaft to fail, as the Von Mises stress reaches 35 MPa, which is very high stress. Although, the deformation all over the shaft is approximately 50mm which indicates that the shaft geometry is under deformed, and size changed. All these parameters result in making the shaft fail to overcome the friction force of the bearing, which results in the shaft moving without being able to move the robot who is fixed to the bearings, thus resulting in shaft deformation.

The shaft position and speed are very important as the shaft is directly connected to the motor and to the robot, so the robot speed and position is the same as the shaft speed and position. In this approach, where the shaft failed to move the robot, it also failed to travel the required distance with the required velocity.

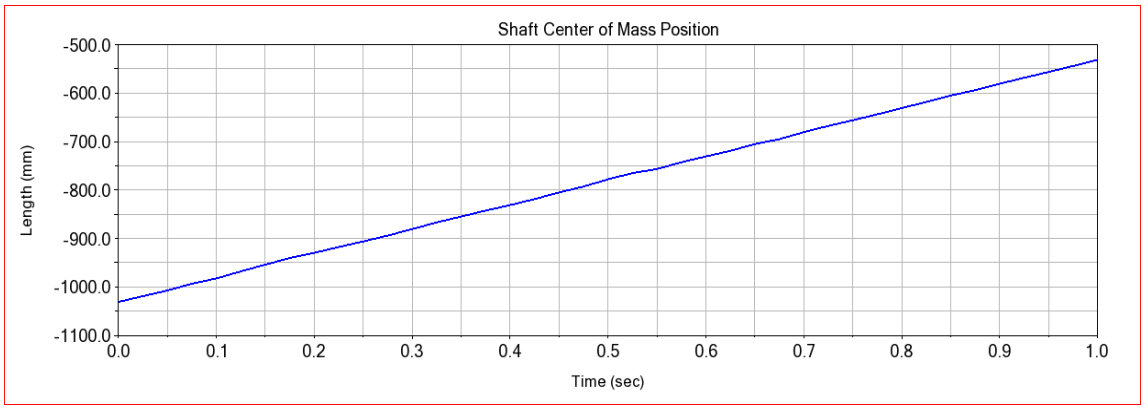

Figure2.4 Shaft Position Curve

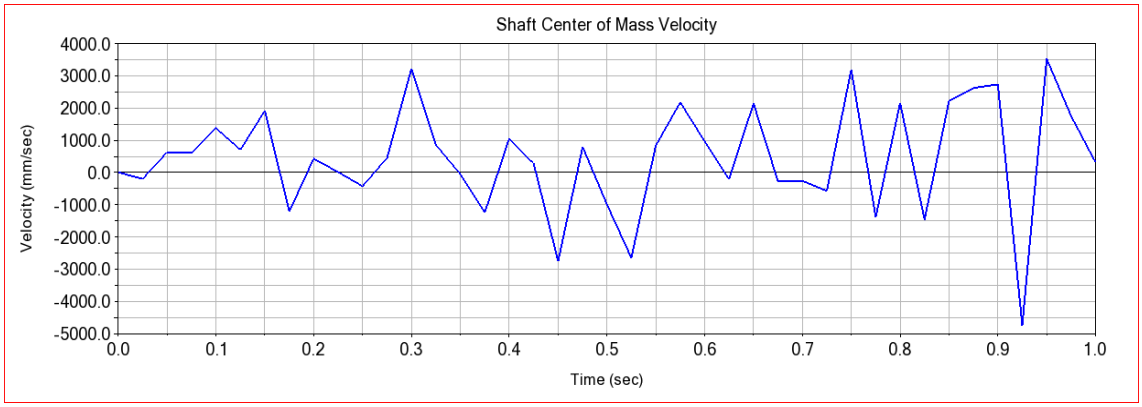

Figure2.5 Shaft Speed Curve

As it appears in figures (2.4) and (2.5), the shaft has travelled only 500mm while it should be 950mm, same for the velocity. The velocity curve shows that the shaft accelerates and decelerates randomly; thus, resulting in high torque required to rotate the shaft. The velocity is also not in the desired range as the shaft speed should be 1500mm/s at max. All these parameters reflect the fact that transmitting the motion to the robot from one axis will lead to shaft, and operation failure.

Two Axis Transmission Approach

After the failure in the one axis transmission, another approach should be found to transmit the motion properly. The two-axis transmission is designed to transmit the motion from the motor to the shaft in which transmits it to the robot. This approach is transmitting the motion to the robot from the 2 ends of the robot (where the bearings are), this will result in decreasing the moment about the rotation point as now the rotation is transmitted next to the bearings. This approach has a very good result, as the shaft is performing its function properly with the desired speed and moving to the desired position. Moreover, as the below figure states, the stress on the shaft is reduced to 27MPa at maximum when the robot approaches the end point. These results show that the 2-axis transmission is safer for the shaft than that of only having 1 axis, additionally the performance of the robot has become approximately as it desired to be.

VON MISES Hot Spots for connecting_rod_flex Date= 2023-04-09 23:57:26						
Model= .First		Analysis= Last_Run		Time = 0 to 1 sec		
Top 10 Hot Spots			Abs	Radius= 0 mm		
Hot Spot	Stress	Node	Time	Location wrt LPRF (mm)		
#	(newton/mm**2)	id	(sec)	X	Y	Z
1	26.3736	774	0.914104	324.076	793.86	-285.793
2	24.7408	756	0.914104	326.567	788.829	-285.54
3	23.7899	763	0.914104	326.567	797.579	-285.54
4	23.5711	875	0.914104	325.61	793.86	-276.114
5	23.2287	711	0.823607	321.035	793.859	-277.87
6	21.2664	877	0.914104	326.866	788.829	-276.491
7	21.2049	772	0.914104	322.852	800.223	-285.431
8	20.3547	881	0.914104	327.465	788.829	-275.17
9	20.2513	776	0.914104	322.819	788.829	-285.416
10	20.2019	698	0.914104	322.22	788.829	-286.737

Figure2.6 The most 10 nodes in the shaft that are subjected to stress.

For the operation the shaft is successfully traveled from the beginning to the end of the shelf. Figure (2.7) shows the same input values that are used to evaluate the first approach, but with lower parameters, that means this design is better than who has only one axis.

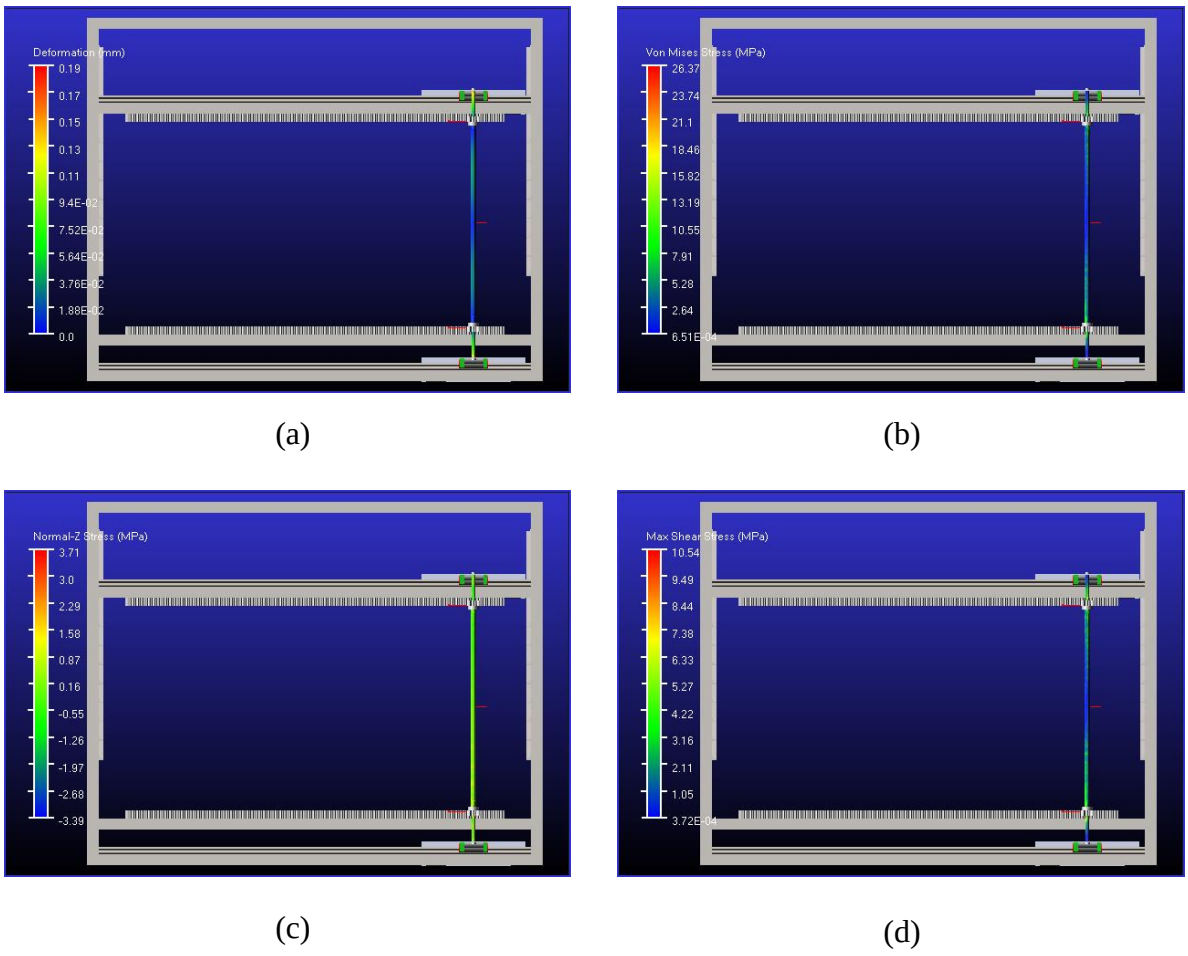

(a) (b)

(c) (d)

Figure2.7 (a) Deformation, (b) Von-Mises Stress, (c) Shear stress in z direction, and (d) Max shear stress

The deformation is decreased to be 0.018mm instead of 50mm, the other parameters such as the shear and Von Mises stress are decreased, and distributed all over the shaft, so the shaft has no points of high stress, while other points are subjected to low stress, which means the stress on the shaft is homogeneous.

In addition, as figure (2.8) shows, the position curve of the robot while moving from one point to another, the robot decelerates when approaching the end point not as in one axis approach the robot keeps moving in constant speed; thus, result in very high deceleration when the robot reaches the end point, which will result in high torque requirement of the motor to stop the robot.

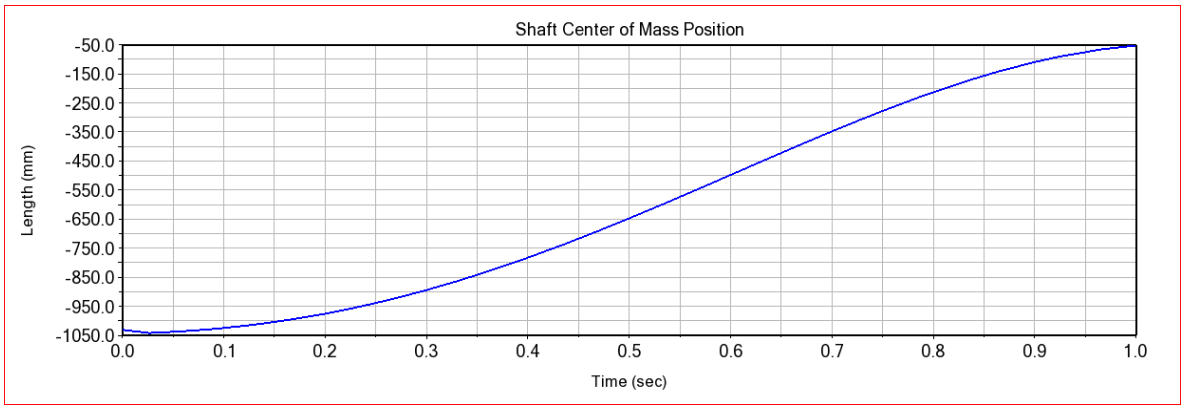

Figure2.8 Shaft CM position in mm

the speed curve shows the ideal behavior that the robot should take, as the speed is increasing and decreasing gradually, there is no sudden change in the speed so the acceleration is constant in this case; thus, would result in zero jerk which will keep the robot away from vibrations and failures.

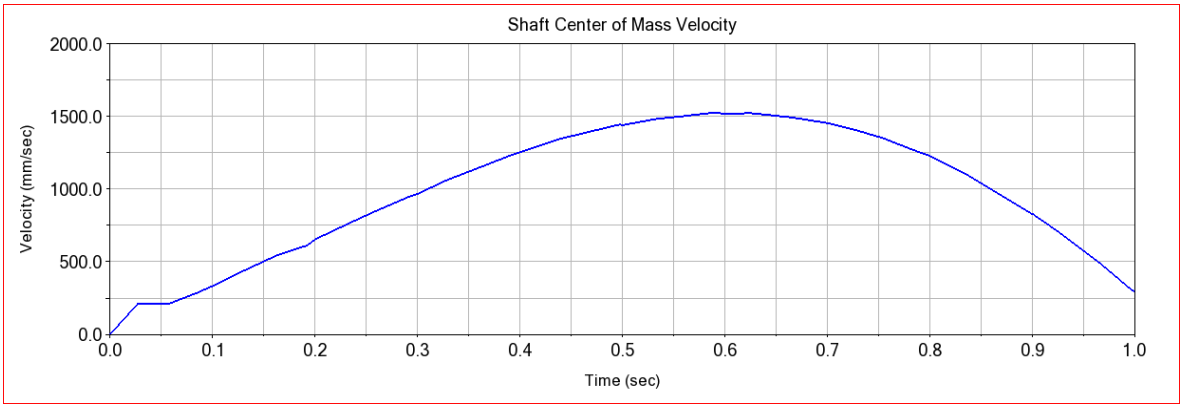

Figure2.9 Shaft CM Speed in mm/sec

2.1.6 Proposed Design

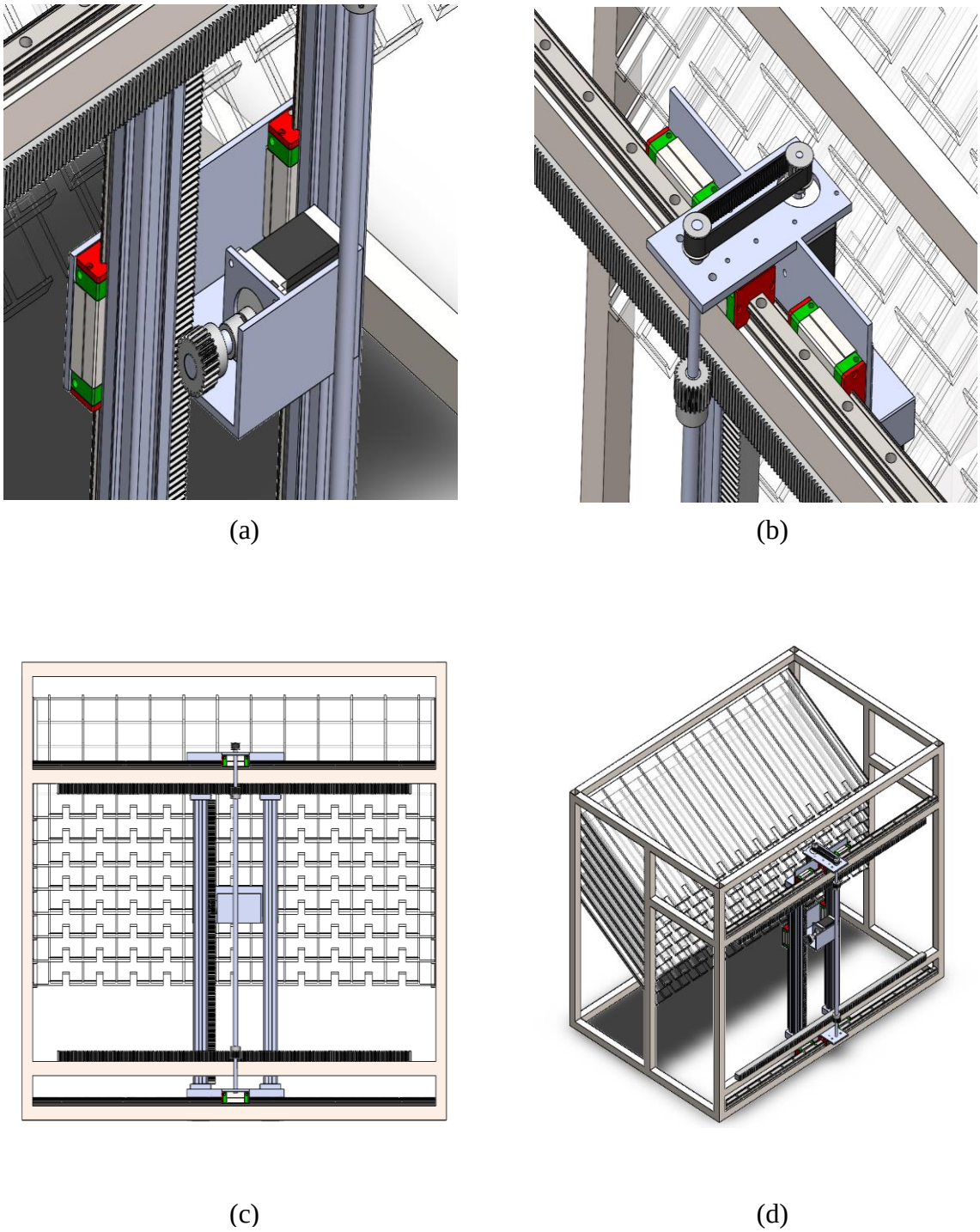

(a) (b)

(c) (d)

Figure2.10 Proposed Design, (a) Y-axis, (b) X-axis, (c) Front View and (d) Isometric

2.1.7 Machine Parts

Given that the robot's design aims to be as quick, compact, and affordable as feasible, the system's components and design have been chosen to meet the project's objectives. The design's parameters and dimensions are listed below.

System Frame

Since the robot is incorporated onto the shelf, the frame's design aims to reduce the system's floor space as much as possible. The robot's cartesian motion compelled the arrangement of the medications to be on a 2D plane on the shelf, allowing the robot to access each one roughly at the same time. The frame is built of steel 37 to increase its rigidity and absorb vibrations brought on by the robot's fast mobility. The use of an aluminum frame would have been an excellent option, but it was rejected because of its high cost.

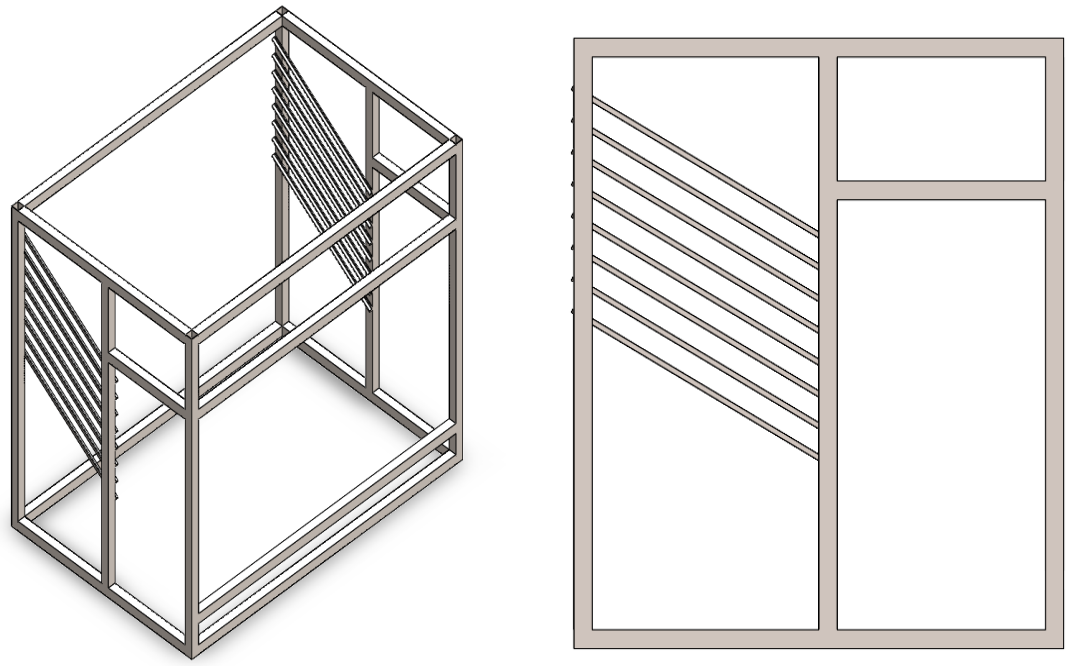

(a) (b)

Figure2.11 System Frame, (a) Isometric View and (b) Side View

To enable the robot to travel down the horizontal axis supported by linear guides, it must be positioned between the two horizontal bars in the front picture (3.11-a). The slanted supports are used to secure the shelves.

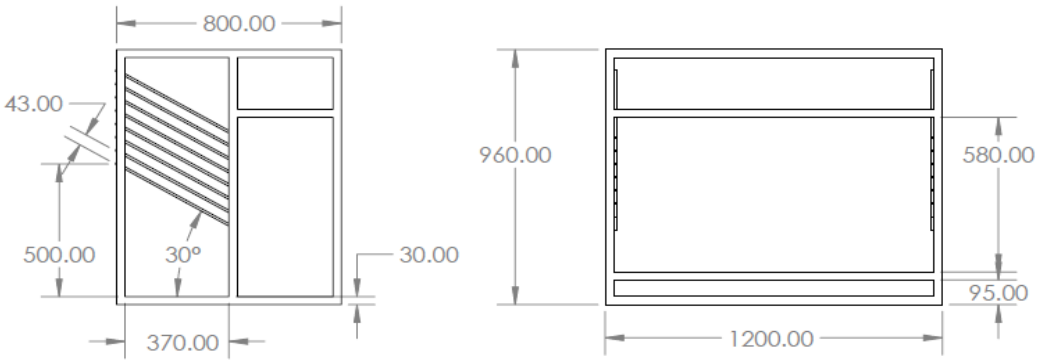

Figure2.12 Dimensions of the Frame in mm

Gravity Shelf

The gravity shelf was chosen for this task because it will prevent medicines from falling off the shelf until the robot arrives to pick them up through a small notch at the end of the shelf that will aid the robot in picking up the drug. The shelf design was made to make the dispensing process easier and faster. According to (Adrián et al., 2019), the angle of inclination is fixed at 30 degrees since this is the angle that will prevent the medications from falling off the shelf or resisting when the robot raises them up to pick them up.

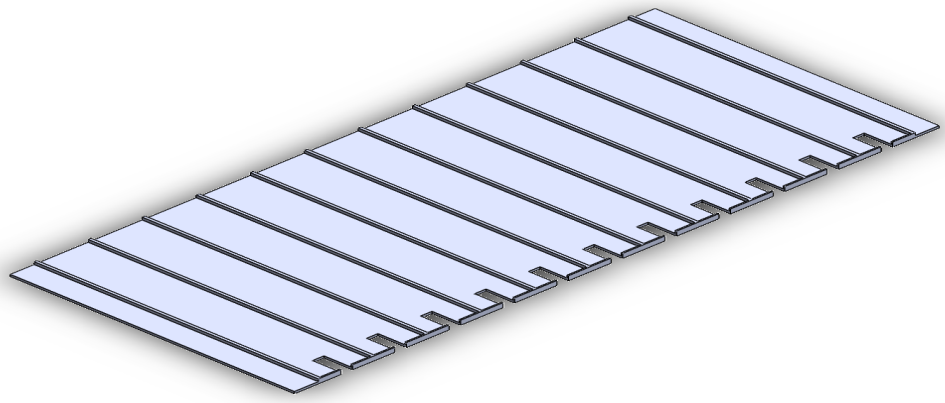

Figure2.12 Isometric View of the Shelf

The shelf is made of 5 mm thick MDF since it is less expensive, lighter than aluminum, and a relatively robust material that is difficult to bend. Low-thickness acrylic would have been the best option for this function and might have been a solution, but it would have been much more expensive than MDF, making MDF the better option. Each shelf has eight channels, each of which may carry one type of drug with a capacity of six to seven packets. There are about 55 drugs that can be stored on each shelf.

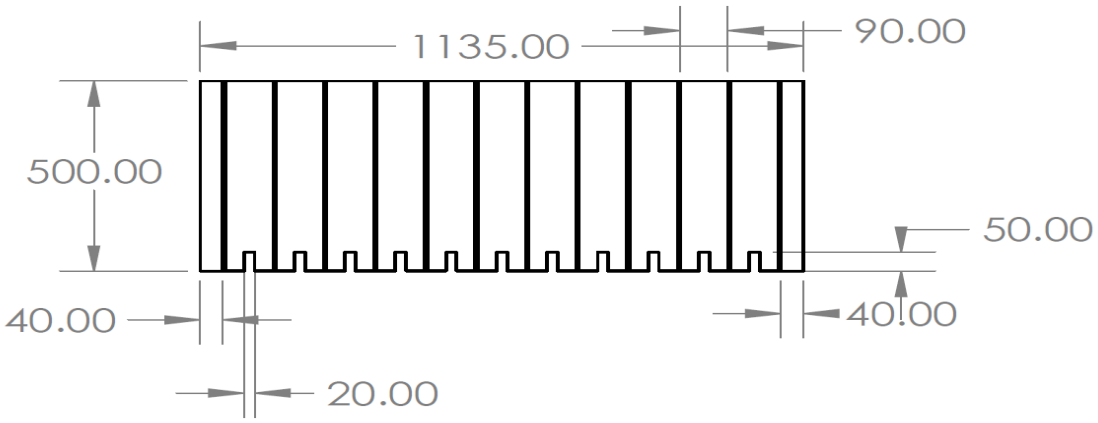

Figure2.13 Dimensions of the Shelf in mm

Motor Holders

An essential component, the motor holder transmits motion from the motors to the robot body while holding the motor firmly in place. Two motor holders and one supporter are used in the design; the supporter's job is to transfer motion from the lower half of the shaft to the lower section of the x-axis, transferring motion to the robot from top to bottom to prevent axis deflection. In order to transmit motion to the axis, all motor holders and the supports are built of 5 mm steel 37. Because they transmit motion to the axis, they must be hard while still being light in order to lower the motor's torque requirements of the motor. Steel 37 was chosen as a replacement for stainless steel because it is heavy and has a poor strength-to-weight ratio. Steel 37 also has better thermal conductivity than stainless steel, which results in better heat distribution. This property is useful because the motor's operating temperature ranges between 100 and 120 degrees Celsius.

X-axis Holder the x-axis motor holder is a T-shaped component, with the right flange holding the motor and fixing it to the axis' linear bearing while the left flange secures the top of the shaft to maintain the contact between the rack and pinion. The purpose of the holder is to keep the motor and shaft in place while also transmitting the linear motion of the shaft to the motor body and the axis. In this way, the robot moves in simultaneously with the motion of the shaft, and the motor moves in simultaneously with the shaft to remain constantly engaged.

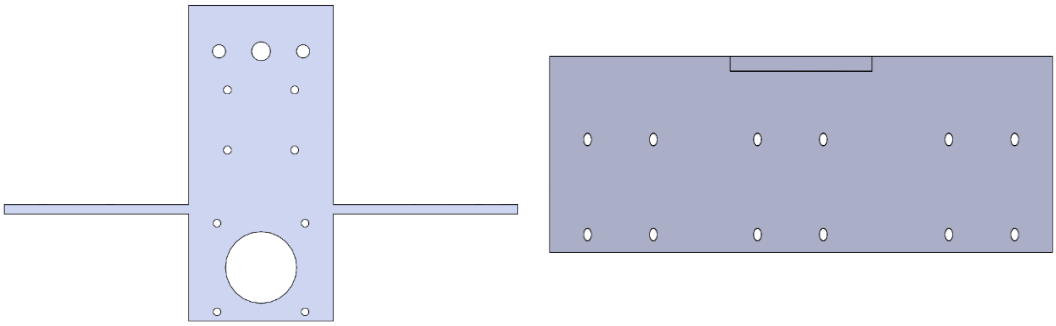

(a) (b)

Figure2.14 X-axis Motor Holder, (a) Top View and (b) Front View

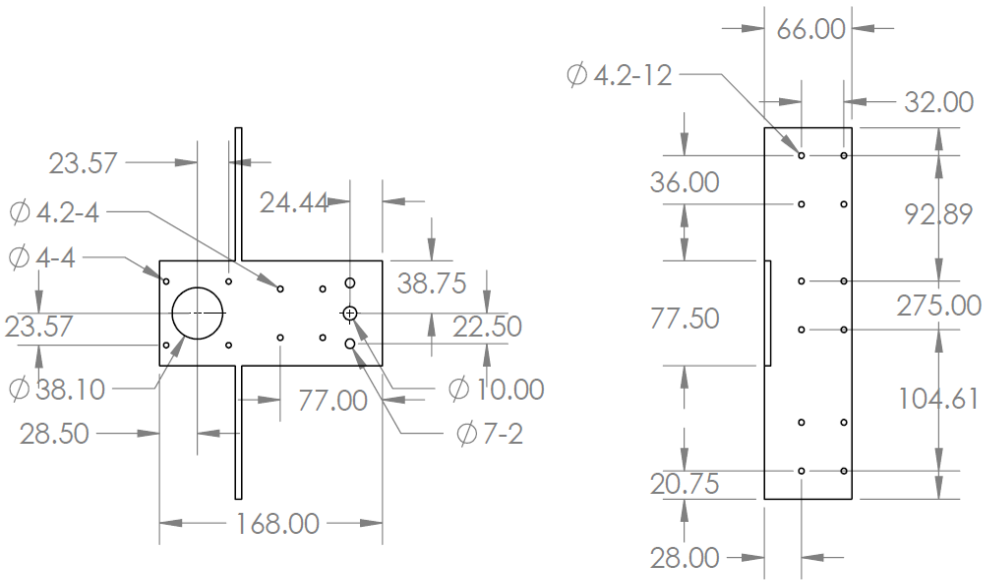

Figure2.15 X-axis Motor Holder Dimensions in mm

X-axis Supporter The supporter's responsibility is to both hold the shaft's bottom and convey its linear motion to the robot's bottom end. The supporter design is an L-shaped component that the shaft's lower end rests on the flange, mounted by a bearing to stop the shaft from sliding on the flange and transfer motion to the robot.

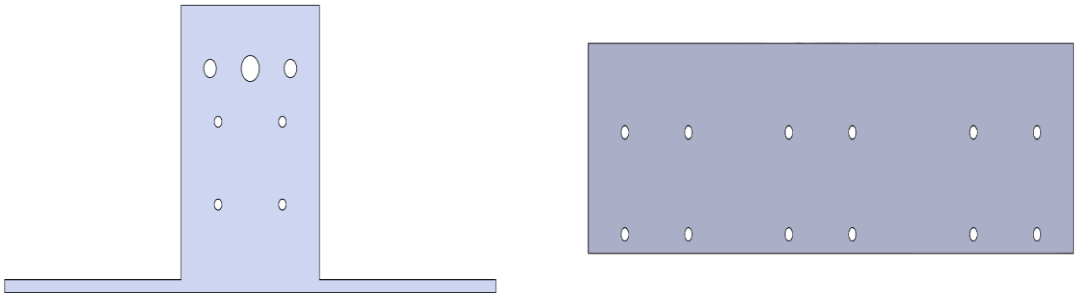

(a) (b)

Figure2.16 X-axis Supporter (a) Top View and (b) Front View

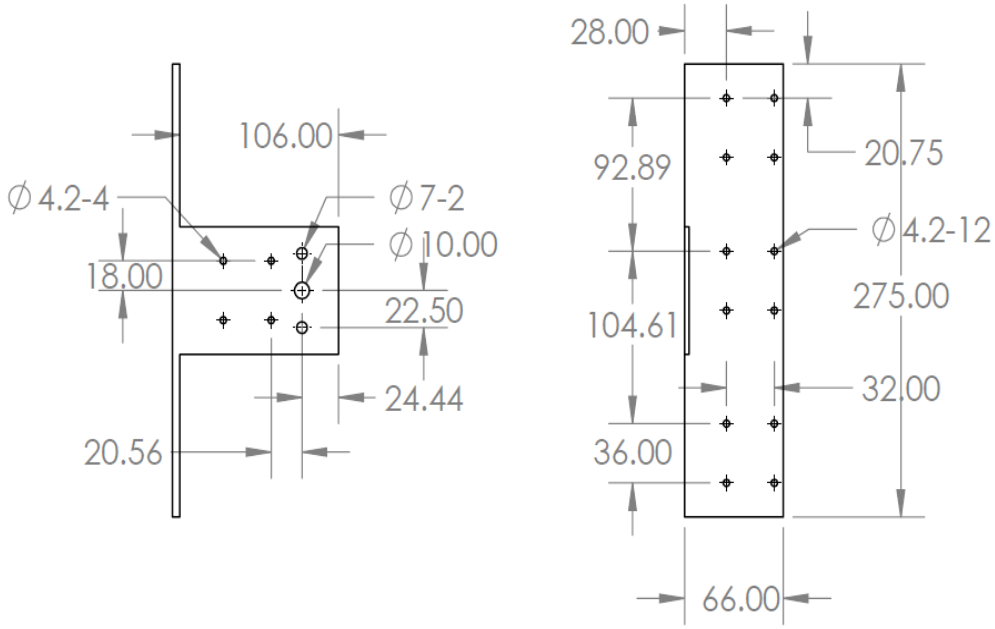

Figure2.17 X-Supporter Dimensions in mm

Y-axis Holder the Y-axis motor holder serves an extremely significant purpose since it transmits motion from the motor to the y-axis and holds the end-effector, which is the component that will dispense the medications. Using screws, the motor is fastened to the component. A pinion connects the motor to the rack, and when the motor is rotated, the pinion moves with the rack, causing the motor to travel linearly up and down. This also causes the y-axis, which is fixed to the motor, to move up and down. The end-effector can be mounted on the axis using the eight screw holes on the part's front.

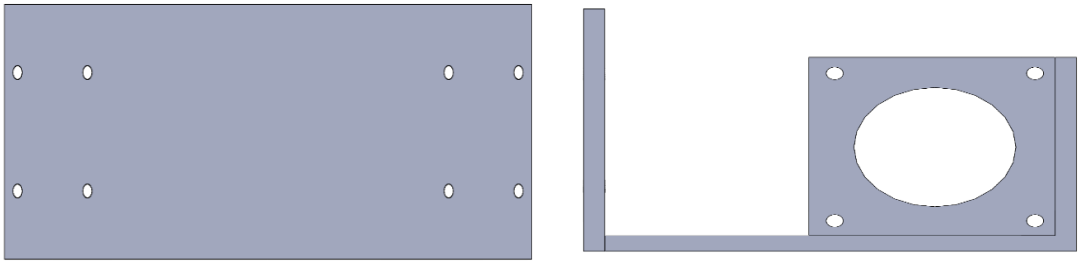

(a) (b)

Figure2.18 Y-axis Motor Holder (a) Front View and (b) Side View

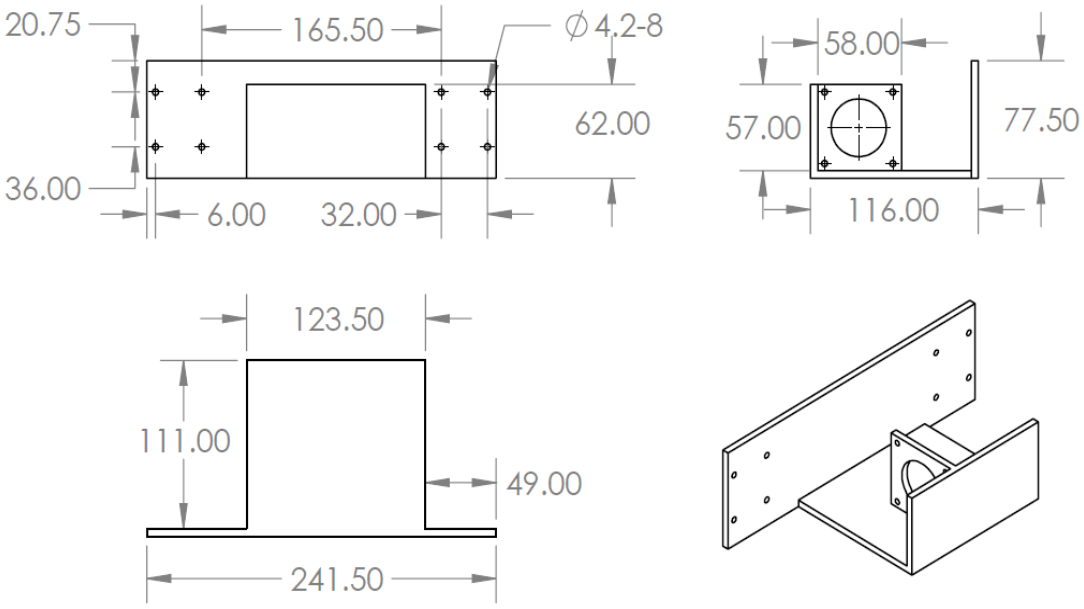

Figure2.19 Y-axis Motor Holder Dimension in mm

End Effector

The end effector is designed to get the medicines from the shelves and dispenses them to the channels where it will be delivered to the customer. Thus, to make sure this process is done perfectly the end effector is constructed of several parts. One of the necessary parts of the end effector is the separator that its mission is to separate between medicines in the end effector's body so that each medicine's barcode is read and identify if this medicine is the ordered one or not. The other parts are three motor holders, one that holds the motor which is responsible for rotating the end effector's body 90° so that it dispenses medicines in channels. Another one is to maintain the motor that is responsible for sliding the medicines at the end effector's body. The last one is responsible of holding the motor that moves the separator up and down. Another important part to the end effector is the support that transmits the motion from the motor to the end effector to rotate the body and also maintain its body with inclined 30° to help medicines slide along the body freely.

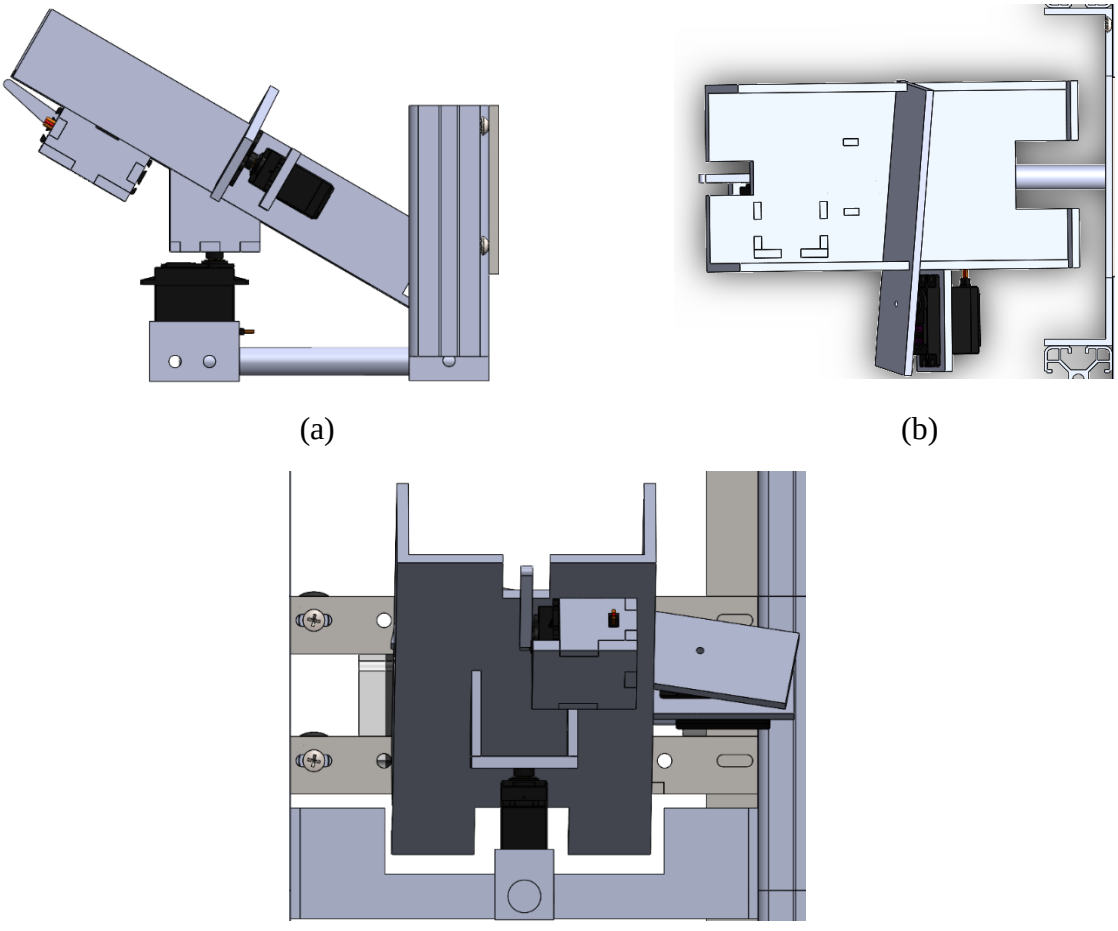

(a) (b)

(c)

Figure2.20 End Effector Assembly, (a) Side View, (b) Top View, and (c) Front View

The end effector is supported by a rod that is fixed by a holder to maintain its stability. This holder is responsible for fixing the end effector to the movable part to receive the same motion of the X and Y directions. This holder is designed to be C-shaped and is fixed to two aluminum profiles by screws. The two aluminum profiles are used as an extension so that the end effector can reach the very last shelf appropriately.

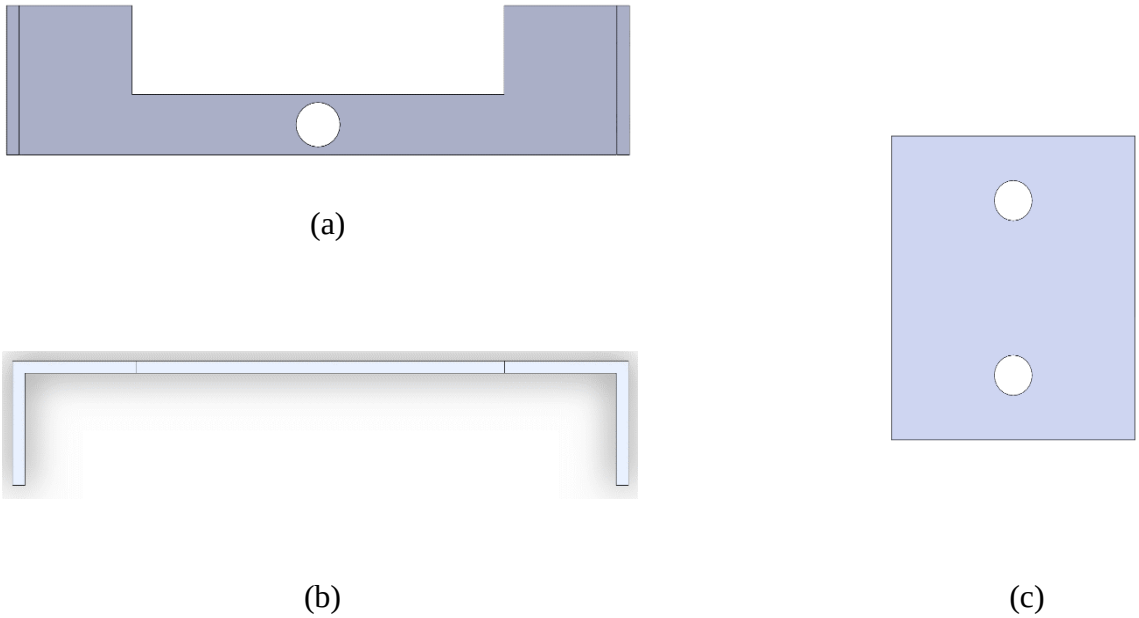

(a)

(b)

(c)

Figure2.21 End Effector Holder, (a) Front View, (b) Top View, and (c) Side View

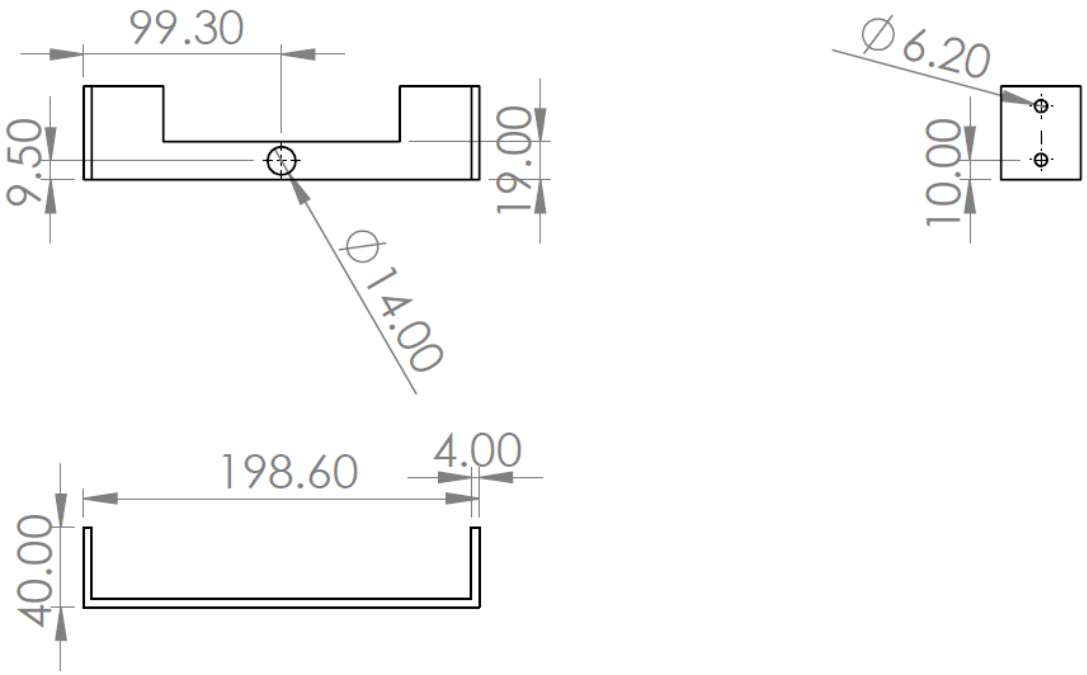

Figure2.22 End Effector Holder Dimensions in mm

The materials of the end effector and its holder is chosen based on some criteria. The materials were chosen to be a combination between metal (steel and stainless steel) and wood (MDF). The holder is made of steel 37 to maintain the rigidity and can sustain the load without bending. Also, the rod that connects the holder and the end effector is made of stainless steel. On the other hand, the end effector's body is made out of MDF so that it is with approximately negligible weight, so it does not add load on the motor and dispense medicines with the required speed. All these criteria were taken into consideration and in addition to this they were chosen to meet the project's budget and with the shortest period of time of machining so that the system could be established on time. A table was made to make a comparison between all the available materials in markets to decide the materials of the end effector.

Table2.1 Comparison of End Effector Materials

Material	**Density in Kg/m^3**	**Mass in Kg**	**Cost of raw material in L.E**	**Cost of Machining in L.E**	**Total Cost in L.E**
MDF Wood	620	0.15	30	40	70
Acrylic	1180	0.24	340	70	410
Aluminum	2700	0.54	100	200	300
Steel	7800	1.56	120	100	220
Plastic	1240	0.25	130	750	880

Shaft

For the design to work, the shaft is a need since it synchronizes the motion of the top and bottom x-axes to prevent deflection. For the x-axis, a synchronization circuit and the use of two motors were replaced with the shaft. Two fixed pinions on the shaft will revolve in tandem with the shaft's rotation when the motor transfers power to it from the top of the shaft through a sprocket and chain. These two pinions, which are situated at the top and end of the shaft and are engaged with two racks, cause the x-axis top and bottom to travel at the same speed and across the same distance when they are both rotating at the same time. The shaft is made of steel since it is readily available on the market and because of its stiffness. To determine the smallest shaft diameter that could be employed without failing or breaking, the shaft design is described in the following section.

Standard Parts

The aluminum profile is used to place the y-axis on, and the end-effector will travel along it. It is utilized because it is simple to install, light in weight, and has high flexibility in fixing parts through its slots. The design includes several standard parts, which are given in table (2.2) below. In addition to supporting the motion of the axes and supporting some of the robot's weight in place of the motors, the linear guides and bearings also help to maintain the stability of the robot. The motion from the motor in the y-axis and from the shaft in the x-axis is transferred to the axes in this design using linear guides and bearings as well. They are very simple to install. Since the axes require linear motion, the RPD is employed to transfer power from the motors to the axes. RPD is chosen because it is quicker than a ball screw and more dependable than a belt drive. It is also particularly useful for long distance travel.

Table 2.2 Standard Parts List

Name	Specs	Image
Aluminum Profile	• 40*40 mm cross section dimensions • 620 mm length	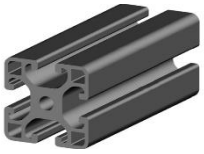 Figure2.23 Aluminum Profile (Datasheet)
Straight Rack	• Module = 1.25 • Width = 22 mm • Height = 23 mm • Length = 1000 mm for X • Length = 600 mm for Y	 Figure2.24 Rack (Datasheet)
Straight Teeth Pinon	• Module = 1.25 • Number of Teeth = 24 • Bore diameter = 12.7 mm • Total length = 32 mm • Keyway = 5 mm*2 mm • Hub diameter = 24 mm	 Figure2.25 Pinion (Datasheet)
Linear Rail	• Model no: HGR25T1200P for X • Model no: HGR25T600P for Y	 Figure2.26 Linear Guide (Datasheet)
Linear Bearing	Model no: HGH25CAZ0P	 Figure2.27 Linear Bearing (Datasheet)

2.2 Components Sizing

Components sizing is very important in such big, and precise projects. Component sizing is done on parts that are subjected to failure, and fracture. Components sizing avoids the failure of parts and makes the operation of these components as functional as possible.

2.2.1 Motor Sizing

In order to maintain the right motion with accurate positions and fastest dispensing; a motor sizing study was made to select the best motor for the required application. The motors positions in the proposed design are shown in figure (2.17), so based on their locations some additional load was added; so, a motor sizing study was made to calculate the load torque for x and y axes.

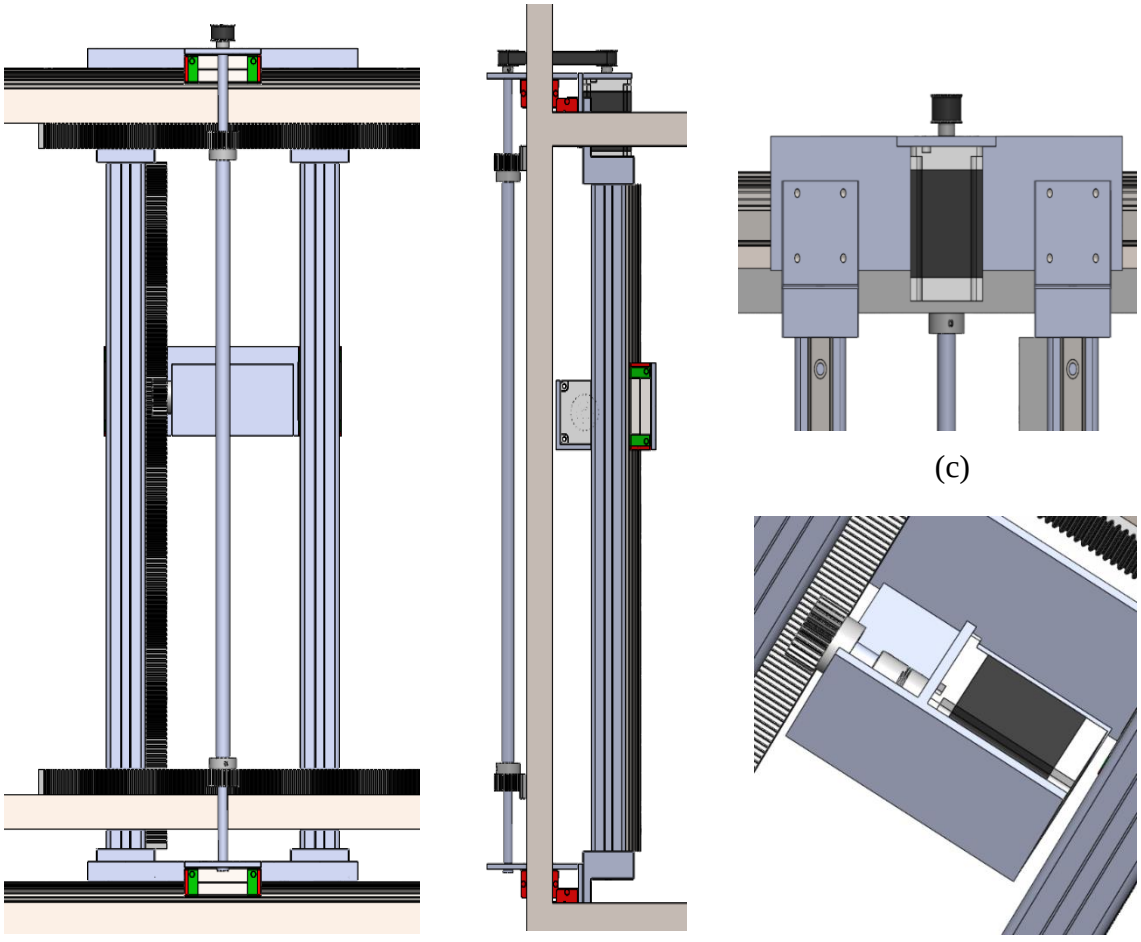

(a) (b) (c) (d)

Figure2.28 Proposed Design Motor Location, (a) Front View, (b) Side View, (c) X-Axis Motor Position and (d) Y-Axis Motor Position

X-axis Motor Sizing

The motor that will be responsible for the motion on x-axis right and left motion, will be heled at top of the bearing with the aid of a T-shape sheet metal that will carry it. After transforming the rotational motion to linear motion, the linear guides are used and added to maintain the robot stability and serve the linear motion with linear guides. In addition to the body that will dispense the medicines, its back will also hold the motor of y-axis; so, that will add an extra load to the motor. Moreover, the masses of the aluminum profile, y-rack, and y-pinion, the three linear bearings and the two pinions will be added to the load held on the motor. To analyze the forces that will act on the motor, a free body diagram of the design must be drawn first.

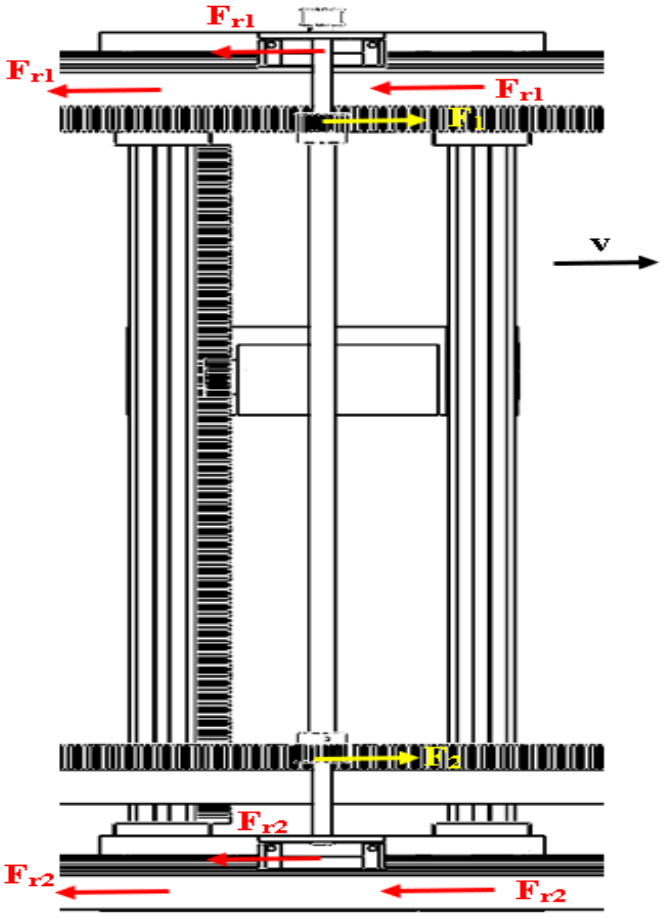

Figure2.29 FBD of X-axis

According to (Atlanta, 2012) the bearings friction reactions were analyzed because the masses weight to be transmitted motion direction is opposite to the linear bearing motion direction so they have reactions as F_r. F is the tangential force that will be substituted with its affecting torque with knowing that the v is the velocity direction. The force analysis was made in order to calculate the load torque.

$$\boldsymbol{\Sigma F = ma} \tag{2.1}$$

$$\boldsymbol{F_1 + F_2 - 3F_{r1} - 3F_{r2} = ma}$$

Table of Overload Factors, K_o

Driven Machine			
Power source	Uniform	Moderate shock	Heavy shock
Uniform	1.00	1.25	1.75
Light shock	1.25	1.50	2.00
Medium shock	1.50	1.75	2.25

Figure2.30 Overload Factor Table (Richard *et al*, 2011)

Adding the factor of safety S = 1.1 and the overload factor K_a = 1 (as both the load and the power source are uniform) to the equation, according to the table of Overload factor (Richard, et al, 2011). Since all the bearings are from the same type; they all have the same friction force, so they were added together to have the following equation.

$$\boldsymbol{2F = (m * a + 6 * F_r) * S * K_a}$$

To calculate the torque on the pinion is simply by multiplying the summation of forces by the pitch radius of the pinion.

$$\boldsymbol{T = 1.07Nm \text{ approximately } = 1.1Nm.}$$

Y-axis Motor Sizing

The motor that will be responsible for the motion on y-axis up and down will be heled at the back of the body that carries medicines with aid of a L-shape sheet metal that will carry it and the linear bearings mounted on the linear guide on the two-aluminum profile. The motor shaft will be directly connected to the pinion with motor shaft and bearing that will transmit the motion to the body. So, the forces that will act against this motor and make load consisting only of the pinion mass, body of robot mass, L-shape

sheet metal mass, two linear guides mass and the mass of motor. Drawing the free-body diagram to analyze the forces.

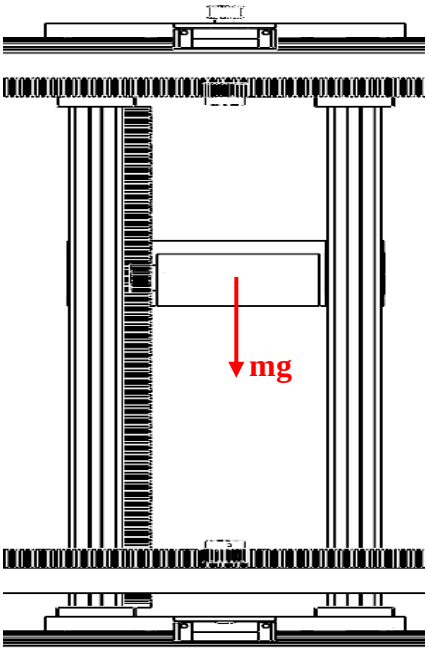

Figure2.31 FBD of Y-axis

Opposite to the motor of x-axis the load now is in the same direction of the guide so there is no friction force due to linear bearings according to (Atlanta, 2012).

$$\boldsymbol{\Sigma F = ma}$$

$$\boldsymbol{F - m * g = m * a} \qquad (2.3)$$

Adding the factor of safety $S = 1.1$ and the overload factor $K_a = 1$ to the above equation.

$$\boldsymbol{F = (m * a + m * g) * S * K_a}$$

Then to calculate the torque required we multiply by the pitch radius of the pinion.

$$\boldsymbol{T = (m * a + m * g) * S * K_a * \frac{d_p}{2}} \qquad (2.4)$$

Using equation (2.4) and by subtituting with the parameters we can find the load torque.

$$\boldsymbol{T = (2.3 * 3 + 2.3 * 9.81) * 1.1 * 1 * \frac{0.03}{2}}$$

$$\boldsymbol{T = 0.49\text{Nm approximatly equals to 0.5 Nm.}}$$

X-axis Motor Selection

To select the best motor for this application the rotational speed at which the motor will rotate must be determined first. So, calculation of the linear distance traveled for the pinion to complete one revolution is done using the following equations.

$$\boldsymbol{d = \pi * d_p} \tag{2.5}$$

$$\boldsymbol{d = \pi * 0.03}$$

$$\boldsymbol{d = 0.094 m/rev}$$

By putting the velocity(v) = 1.5 m/sec, calculating the rotational speed (N) by the following equation.

$$\boldsymbol{N = \frac{v}{d} * 60} \tag{2.6}$$

$$\boldsymbol{N = \frac{90}{0.094}}$$

$$\boldsymbol{N = 958\, rpm}$$

Looking in motors datasheet it was found that the required motor with these aspects is the stepper motor Nema 23 with the serial PL23HS84220 with input voltage of 60v, in order to reach exact position within the required time.

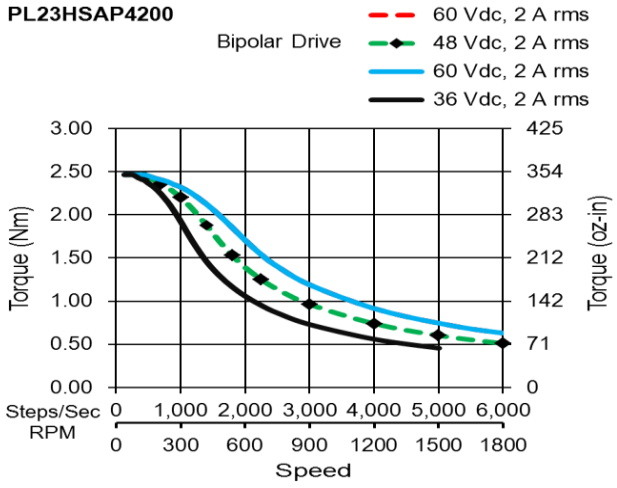

Figure2.32 Torque-Speed Curve for PL23Hs84220 (Motor datasheet)

Y-axis Motor Selection

To select the best motor for this application the rotational speed at wich the motor will rotate must determined first as done for the x-axis motor. As the pinion used for the y-axis is of the same shape as the two pinions used for the x-axis so the distance travelled per revelution will not differ. Although the velcity will be its half because the distance to be travelled by the y-motor is approximately its half (v) = 0.75 m/sec, calculating the rotational speed (N) using equation (3.6) .

$$N = \frac{45}{0.094}$$

$$N = 478.72\ rpm$$

Looking in motors datasheet it was found that the required motor with these aspects is the stepper motor Nema 23 with the serial 57H2P5130A6 with input voltage 48v, in order to reach exact position within the required time.

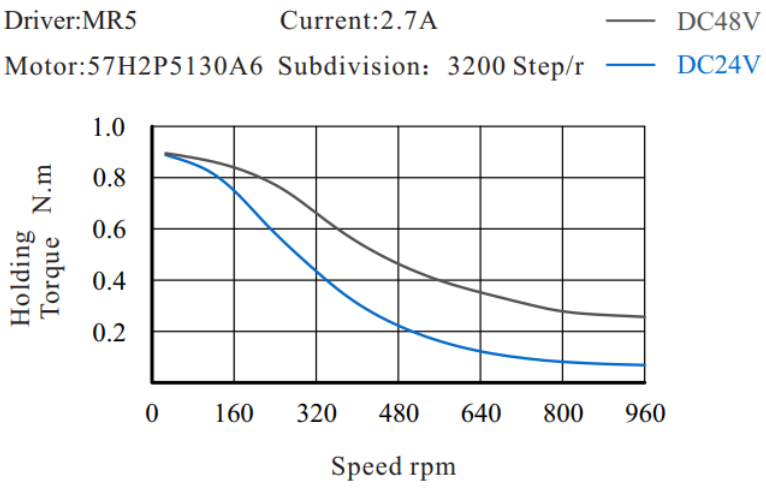

Figure2.33 Speed-Torque Curve for 57H2P5130A6 (Motor datasheet)

2.2.2 Bearing Selection of Shaft

A shaft is used to connect between the two pinions to transmit the rotation motion of the motor where shaft is responsible for the x-axis motion. The motor that is responsible for its motion is held on the top and transmits its motion through a belt and pulley mechanism as illustrated in figure (2.23-b). The motor is fixed on a T-shape metal sheet where the shaft is connected to the pulley through one side and the back of the motor connected to the T-shape holds also the two linear bearings to move smoothly with motion of motor on the linear guide. So, in order to maintain all the requirements of the motion to act properly the shaft must be supported by bearings. Based on the following analysis the bearing is selected.

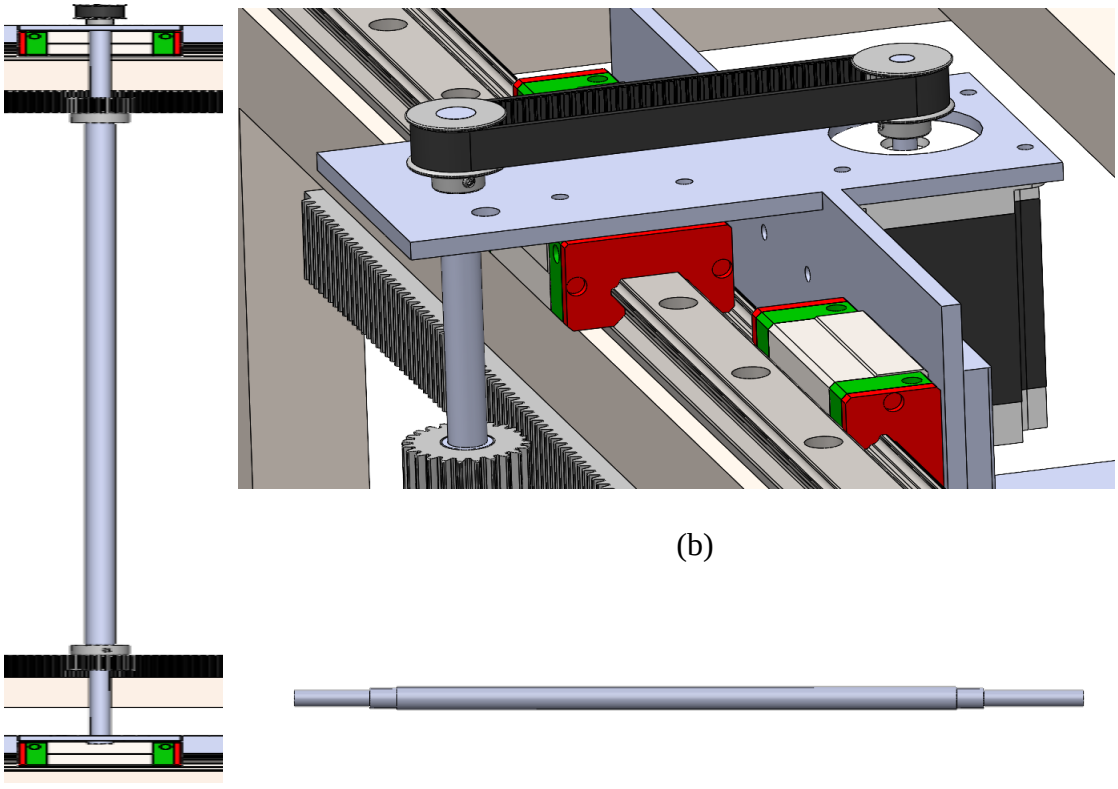

Figure2.34 Shaft Design, (a) Front View of Shaft Connections, (b) Connection of Shaft with the Motor, (c) Shaft

A free body diagram was made to analyze the forces applied to the shaft according to (Richard *et al*,2011).

Figure2.35 Free Body Diagram of the Shaft

where:

- R_{1Z} is bearing1 reaction in Z direction.
- R_{2Z} is bearing2 reaction in Z direction.
- R_{1X} is bearing1 reaction in X direction.
- R_{2X} is bearing2 reaction in X direction.
- R_{1Y} is bearing1 reaction in Y direction.
- F_1 is the tangential force for gear1.
- F_2 is the tangential force for gear2.
- T_1 is the tension force for gear1.
- T_2 is the tension force for gear2.

The force analysis is as the following as the summation of forces equal zero. Where F_1 and F_2 are calculated from equation (3.2) to be equal to 71.56N for each.

$$\boldsymbol{\Sigma F_Z = 0} \tag{2.7}$$

$$\boldsymbol{R_{1Z} + R_{2Z} = 143.3\ N} \tag{2.8}$$

$$\boldsymbol{\Sigma F_x = 0} \tag{2.9}$$

As the tensions in the belt is considered to be negligible a reaction of bearing must be available to maintain stability of the shaft and also allow its rotation along its axis due to the torque applied to it.

$$\boldsymbol{\Sigma F_y = 0} \tag{2.10}$$

Where m is the mass of the whole shaft with all the additional parts on it to prevent slipping the reaction force was needed (knowing that m = 11Kg). The reaction in y-direction is equal to 107.91N.

$$\boldsymbol{\Sigma M_Z = 0} \tag{2.11}$$

$$\boldsymbol{\Sigma M_y = 0} \tag{2.12}$$

$\boldsymbol{\Sigma M_x = 0}$ at point of action of bearing1 reaction (2.13)

With substituting, the second reaction of bearing can be calculated:

$$\boldsymbol{R_{2Z} = 71.56N}$$

From (3.8) the reaction of the first bearing is calculated to be:

$$\boldsymbol{R_{1Z} = 71.56N}$$

From analyzing all the forces that acts on the shaft it is observed that the shaft needs two bearing one acts as a journal bearing at the top of the shaft and the other acts as a thrust bearing. The two bearings are considered to be flanged bearings.

Figure2.36 Flanged Bearing

From the above equations it is observed that the only forces that acts on the shaft are tangential. So, to calculate the minimum diameter to design the shaft the material of the shaft is detected first. It is selected to use steel 47 to design the shaft; the code of steel 47 is "ASTM A29, grade 6150". The approach used for this calculation is the ASME code equation because it takes into consideration both bending and torsion moments applied to the shaft and it is an important approach for the design of transmission shaft. So, the calculation and shaft diameter determination were made based on substitution in the following equation.

$$\boldsymbol{D^3 = \frac{16}{\pi * \tau_{all}} (\sqrt{(K_m * M)^2 + (K_t * T)^2})} \tag{2.14}$$

Where:

- D is the minimum allowed shaft diameter.
- τ_{all} is the allowable shear stress.

- K_m is the bending factor for shock and fatigue.
- K_t is the torsion factor for shock and fatigue.
- M is the maximum bending moment.
- T is the torque applied on the shaft.

The factor of shock and fatigue K_m and K_t are 1.5 and 1 respectively according to the table in figure (2.27), (as the load is gradually applied) according to the mechanical design book (Richard *et al*, 2011). From the mechanical properties of materials table, the yield stress and the ultimate stress of shaft material is 415MPa and 670MPa respectively. Knowing that the allowable shear stress must be 30% of the yield stress and does not exceed 18% of the ultimate stress; the allowable shear stress is calculated to be, $\tau_{all} = 120\text{MPa}$ for a shaft without keyway.

Application	Bending Factor (kb)	Tensional Factor (kt)
Load Gradually Applied	1.5	1
Load Suddenly Applied (Minor Shock)	1.5-2.0	1.0-1.5
Load Suddenly Applied (Heavy Shock)	2.0-3.0	1.5-3.0

Figure2.37 Combined Shock and Fatigue Factors (Girish *et al*, 2015)

The following substitution will be considered as the last step into calculating the minimum shaft diameter.

$$\boldsymbol{D^3 = \frac{16}{\pi * 120}(\sqrt{(1.5 * 0)^2 + (1 * 1070)^2})}$$

$$\boldsymbol{D^3 = 45.41}$$

$$\boldsymbol{D = 3.5\ mm.}$$

The minimum diameter of the shaft must be 3.5mm, adding 5mm for safety, and by approximation D = 9mm.

2.3 Manufacturing Process

In order to make the desired design many manufacturing processes were made. Although, the proposed design was edited by separating the outer frame into two frames one that holds the shelves and the other holds the moving mechanism as shown in figure2.27. This edit was made to meet the project requirements for strengthening the structure of the frame and making it more stable. To manufacture the new design the design went through different phases such as the assembly of outer frame, assembly of the x-axis mechanism and the assembly of the y-axis.

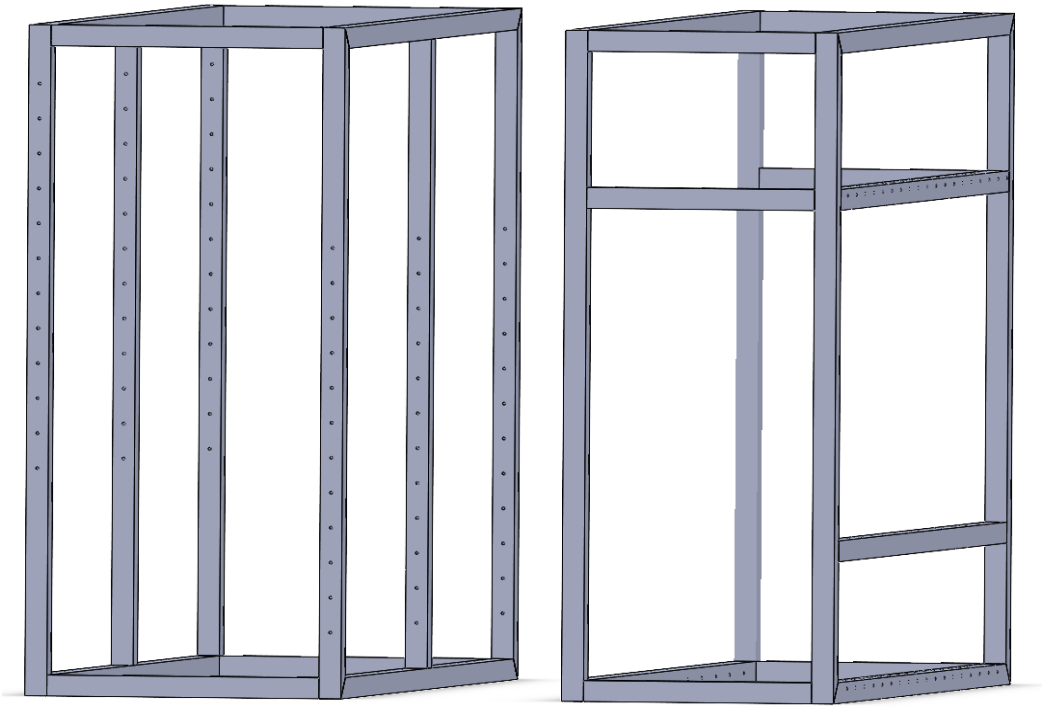

Figure2.38 Edited Frame

2.3.1 Assembly of Outer Frame

This phase began by purchasing the required steel tubes that is machined and cut with the required dimension to complete the whole frame. The tubes were cut with angle 45^0 for the corners and 90^0 for any other part as shown in figure2.28(a). Those tubes were then drilled to make suitable holes that will hold the components that will be added to the frame either the front or the back frame with screws. To make sure that the holes were aligned and in their accurate position a reference MDF plates were cut by laser cutter marking the wholes' locations as in figure2.28(c). Also, after all these processes the tubes were added to be welded together with high accuracy using 90^0 magnetic supports to make sure that the frame was assembled with the same designed dimensions. These processes assured that the frame was accomplished with high accuracy and as required.

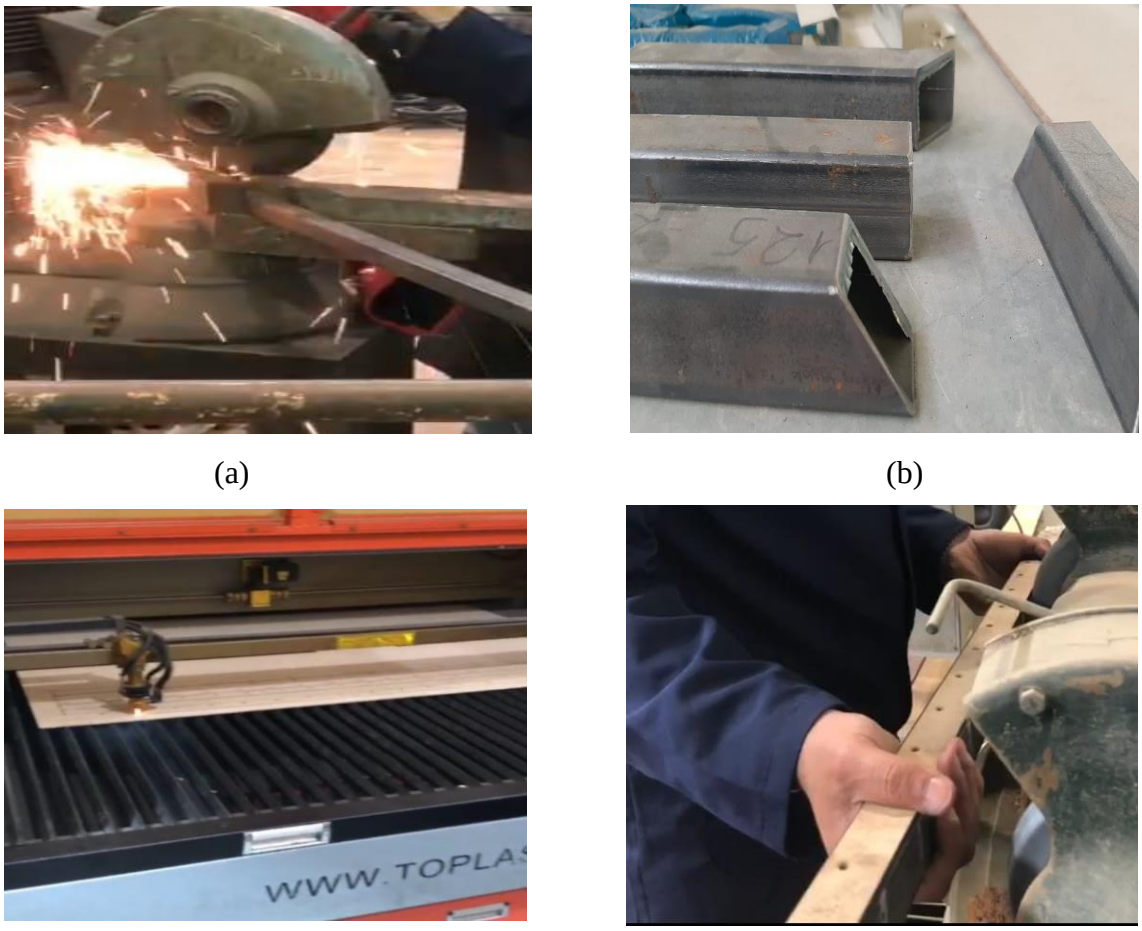

(a) (b)

(c) (d)

Figure2.39 Manufacturing Processes, (a)Cutting Process, (b)Sample of the Cut Tubes, (c)The Reference MDF Plates, and (d)Finishing Machining on the cut Tubes

The welding process was made through phases by welding each face of the frames and then connect them together.

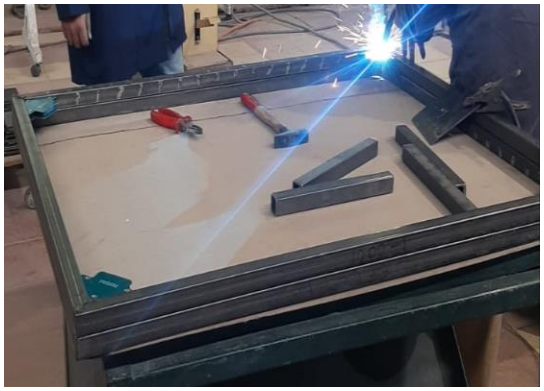

(a)

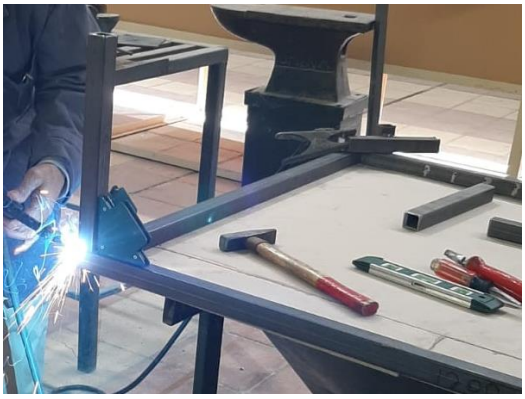

(b)

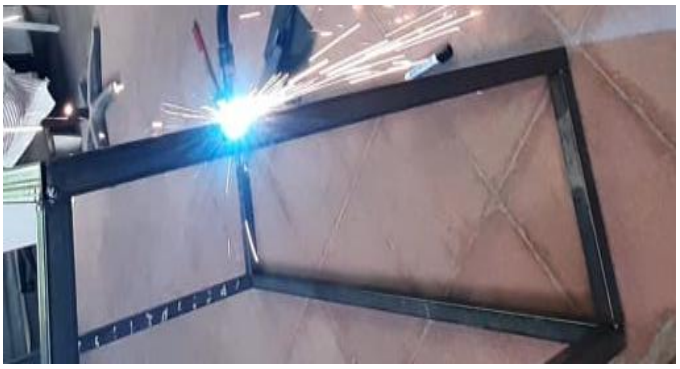

(c)

Figure2.40 The Welding Process, (a)Welding the Frame, (b)Welding the Connectors, and (c)Welding Rest of Parts' Supports

After all these processes the two frames were ready to hold the additional parts that will be added.

(a)

(b)

Figure2.41 The Outer Frames, (a)Front Frame, and (b) Back Frame

2.3.2 Assembly of the X-Axis

This was the second phase of manufacturing. This phase began by purchasing the additional parts as well; the purchased parts are the two racks and pinions, the rails, the linear bearings, the flanged bearings and the required screws and nuts for fixing all of these elements. After installing all of these parts each in its exact position, the motor holder and connector was manufactured and installed to complete all the requirements for the x-axis motion.

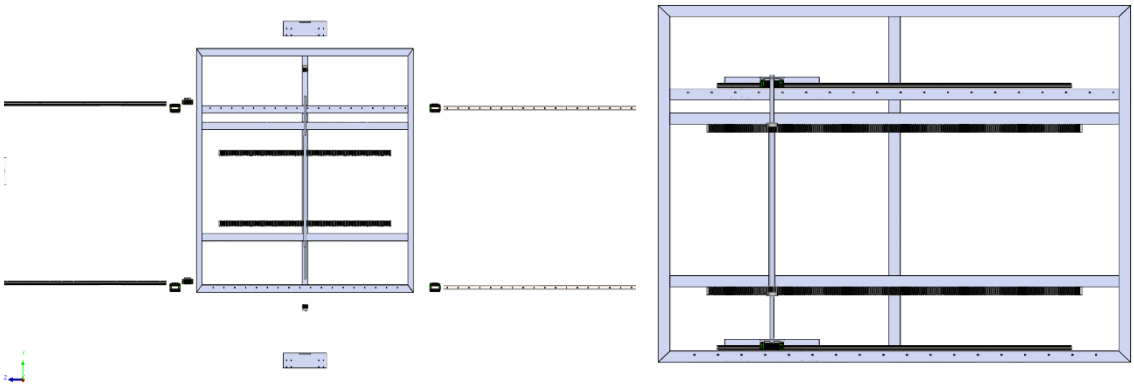

(a) (b)

(c)

Figure2.42 The X-Axis elements, (a)3-D Model of the Frame and Components, (b)The Assembled 3-D Model, and (c) Real Assembled Frame and X-Axis Components

Chapter III
Control Methodology

3.1 Preface

This chapter models the system from the control point of view. The chapter consists of modeling the two factors that are used to control the system parameters, the position of the robot which will be determined from the inverse kinematics equation of the robot, and the velocity that is function in the pulse rate. These two parameters should be controlled to assure the best performance of the robot.

3.2 Robot kinematics

This section consists of the way the distances is calculated to reach the required location. To get the inverse kinematics of the system, the forward kinematics of the system must be analyzed first because it is responsible for getting the position of the end effector relative to the ground, then observing the equations of the joint variables.

3.2.1 Forward Kinematics

The forward kinematics calculation begins with the frame attachment for the variable joints. As the robot is a cartesian robot so the variable joints are prismatic joints only where the joints are just sliding along the axis of motion as per (John, 2005).

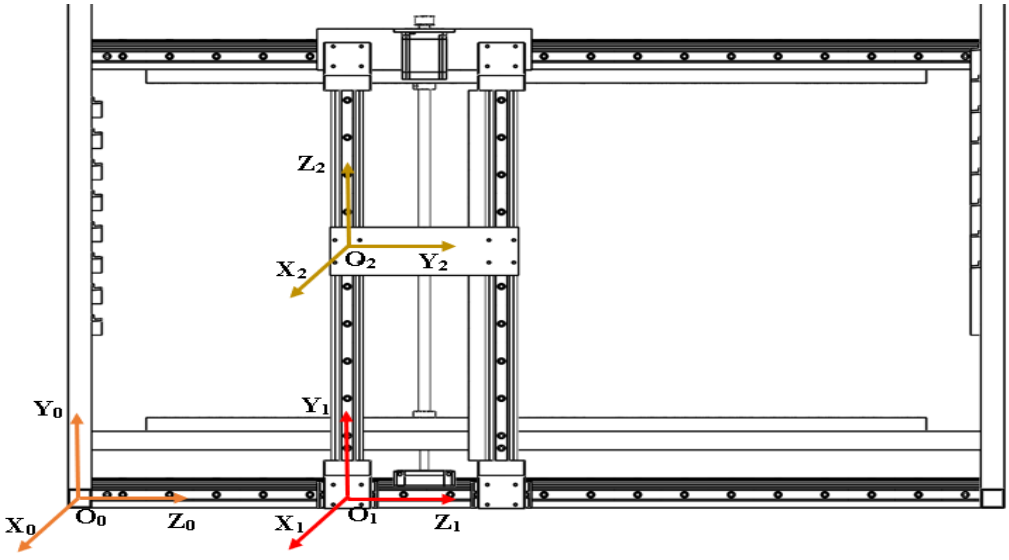

Figure3.1 Frame Attachment of the System

The frame attachment is done based on some rules and as the end effector has no joint, so the second joint is considered as the required final position. The z-axis is first placed based on the direction of the variable joints where in this case are translation motions. The origin is then put based on the joint and the x axes are placed based on the intersections of z-axes of the next joint to be observed. The link zero is the fixed link that does not have a joint and where the transformation matrix begins. The origin of the zero link is placed at a distance as considering the first joint to be at a certain position. To get the forward kinematics the transformation matrix to the end effector must be calculated. The transformation matrix generally consists of 4*4 matrix where the first 3*3 is the rotation matrix where all rotations are needed to reach the end position is calculated of each direction; and the last column represents the position, where the last row of the transformation matrix is zeros except for the last one where it is the scale of the system calculation, and it is 1.

$$ {}^{0}_{2}\boldsymbol{T} = {}^{0}_{1}\boldsymbol{T} * {}^{1}_{2}\boldsymbol{T} \tag{3.1} $$

Where the transformation to the second joint (which is considered to be also the position of the end effector) is to be calculated by multiplying the transformation matrix from link 0 to link 1 by the transformation from 1 to 2.

$$ {}^{0}_{1}\boldsymbol{T} = \boldsymbol{trans}(\mathbf{0}, \mathbf{0}, \boldsymbol{d_1}) \tag{3.2} $$

$$ {}^{1}_{2}\boldsymbol{T} = \boldsymbol{Rot}(\boldsymbol{x}, \mathbf{90}) * \boldsymbol{trans}(\mathbf{0}, \mathbf{0}, \boldsymbol{d_2}) \tag{3.3} $$

The transformation matrix of link one consists only of the translation with distance $d_1$that the robot moved with the first joint. The second transformation consists of a rotation about the x-axis to orient the z-axis to be in the same direction as the one of the second joint then the translation to reach the final joint by distance d_2.

$$ {}^{0}_{2}\boldsymbol{T} = \begin{pmatrix} \mathbf{1} & \mathbf{0} & \mathbf{0} & \mathbf{0} \\ \mathbf{0} & \mathbf{0} & \mathbf{-1} & \boldsymbol{-d_2} \\ \mathbf{0} & \mathbf{1} & \mathbf{0} & \boldsymbol{d_1} \\ \mathbf{0} & \mathbf{0} & \mathbf{0} & \mathbf{1} \end{pmatrix} $$

This transformation matrix describes the rotations to reach the end position in addition to the final position that is shown in the last column which is then used to obtain the inverse kinematics equations.

3.2.2 Inverse Kinematics

The inverse kinematics of the robot is calculated to get the right position distance so the robot can reach every medicine location with specific distances ordered to it. From the forward kinematics transformation matrix, the position matrix is observed to be as follow.

$$ {}^{0}_{E}\boldsymbol{P} = \begin{pmatrix} \mathbf{0} \\ -\boldsymbol{d_2} \\ \boldsymbol{d_1} \\ \mathbf{1} \end{pmatrix} \tag{3.4} $$

Each row in the matrix represents the position point in the corresponding axis.

$$ \boldsymbol{X} = \mathbf{0} \tag{3.5} $$

$$ \boldsymbol{Y} = -\boldsymbol{d_2} \tag{3.6} $$

$$ \boldsymbol{Z} = \boldsymbol{d_1} \tag{3.7} $$

Where it is observed to be that the points coordinates will be the required distances to be travelled by each manipulator joint to reach the required location coordinates as showed in the last two observations, considering the z-axis which represent the x-axis in the in the system coordinate system, and the y-axis represents the y-axis in the robot coordinate system.

Substitute d from eq (3.5), then add the current position to the equation in terms of calculating the absolute distance that the robot needs to move, that would result in following equations (negative indicates for the direction so it is neglected).

$$ \boldsymbol{Y} - \boldsymbol{P_c} = \boldsymbol{\pi} * \boldsymbol{d_p} $$

$$ \boldsymbol{Z} - \boldsymbol{P_c} = \boldsymbol{\pi} * \boldsymbol{d_p} $$

Where $\boldsymbol{P_c}$ indicates for current position. Now substitute with the new position coordinates to calculate each motor number of revolutions needed to move such a distance.

$$ \boldsymbol{Y\ Motor\ Revolutions} = \boldsymbol{\pi} * \frac{\boldsymbol{d_p}}{\boldsymbol{Y} - \boldsymbol{P_c}} \tag{3.8} $$

$$ \boldsymbol{X\ Motor\ Revolutions} = \boldsymbol{\pi} * \frac{\boldsymbol{d_p}}{\boldsymbol{Z} - \boldsymbol{P_c}} \tag{3.9} $$

3.3 Frequency Generation

The parameter that is the most important to control the motor speed is the pulse rate (Frequency), as the frequency increase the motor speed increases as well. The control of the motor speed will give the ability to control the robot speed, acceleration, torque, and the position as well. The linear velocity directly changes with the frequency, acceleration changes with the rate of change in velocity, so by controlling the velocity the acceleration and deceleration are to be controlled. Moreover, Acceleration is function of torque equation, so that will lead to control the motor torque. Finally, the position can be reached be generating a sequence of different frequencies that will result in moving the robot with certain speed at specific time. To understand the behavior of the robot when applying certain frequency at the motor, first we should see the effect of the frequency on the robot motion parameters.

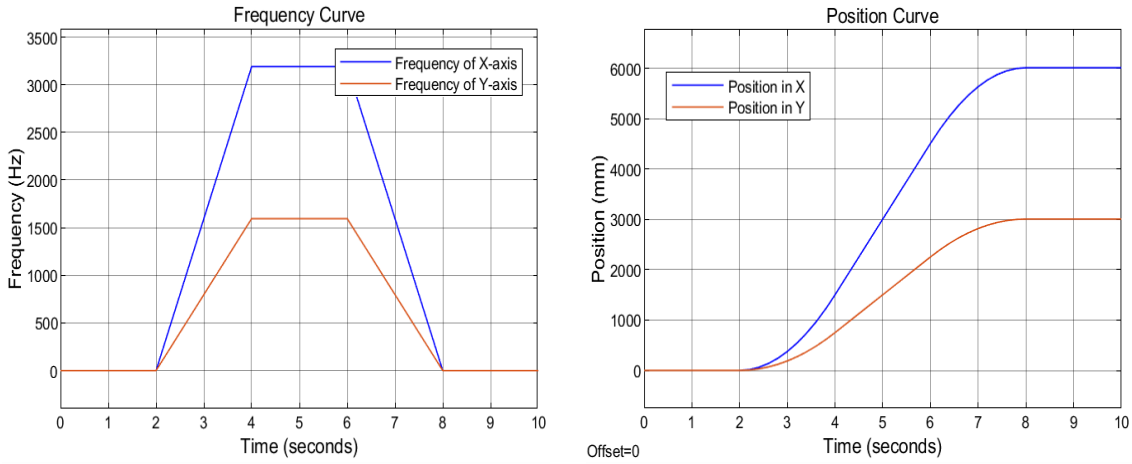

(a) (b)

Figure3.2 (a) Frequency Curve and (b) Position Curve

The graphs in figure (3.2) shows the change in position with respect to the frequency (frequency of the pulses), but since the frequency is too high where the graph will not show the change clearly, so it is represented by a curve with the value of the pulse's frequency appears in the y-axis of the graph. The graphs show how the change in the frequency changes the position as well, with different in amplitude between x, and y-axis but the same curve. The next step is to find the frequency curve that result in traveling the axis from the beginning to the end in both axes.

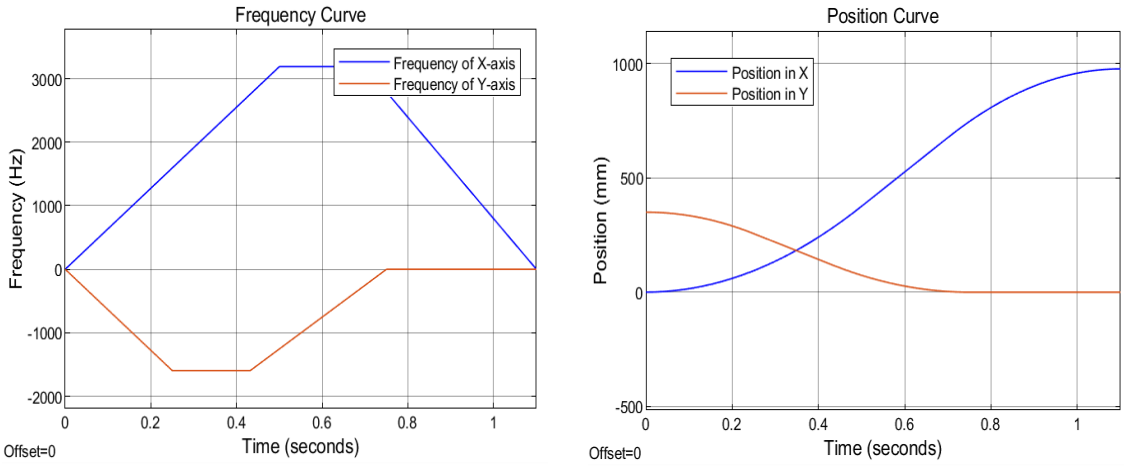

(a) (b)

Figure3.3 (a) Frequency Curve and (b) Position Curve

The graphs in figure (4.3) shows the typical curves for traveling from the beginning to the end of the axes, in both x, and y, but with difference in the time applied as the y curve needs less time to reach the end position; even though y motor speed is half of the x, but y total traveling distance is one third of that of the x. These 4 graphs are very important in path generation, as the frequency curves will be fitted to obtain an equation to fit that curve, same for the position curve. These equations will be used then to calculate the distance that the robot needs to move to reach the desired position. The position's graphs show the operation of moving from zero position to end position and vice versa, as well as frequencies' curves. To solve the problem of frequency generation, 8 equations are needed, 4 for each axis. The first equation is the frequency curve for moving in the positive direction, another one is for moving in the negative direction. The other 2 equations are for position curve moving in both directions, the other 4 equations are the same but for y-axis. The equation used to draw the fitting curve is the sum of sine with normalized values of time to reduce the values of the equation coefficients. The equation

for all curves is the same which is the sum of sine but with different orders and coefficients values.

$$f(t) = \sum_{i=1}^{n} a_i * sin(b_i * t + c_i) \tag{3.10}$$

where n represents the order of the equation.

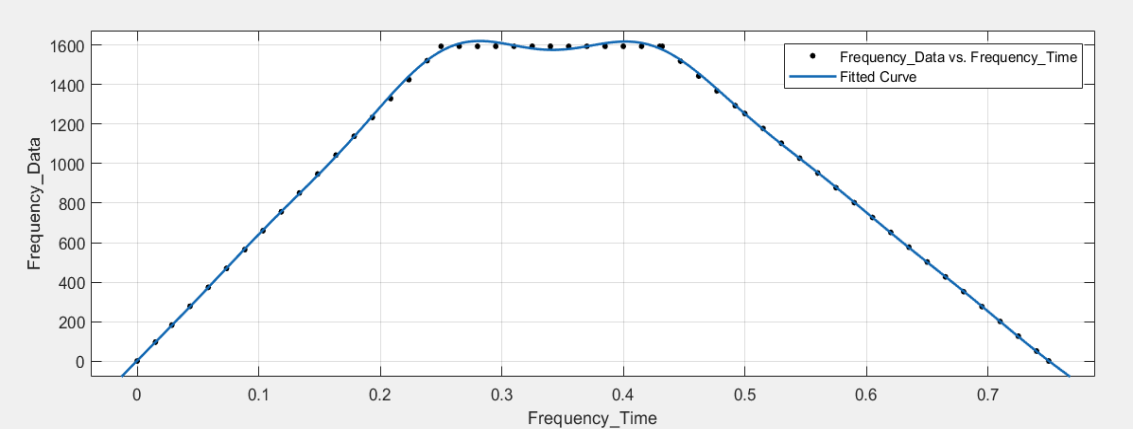

Figure3.4 Frequency Curve Fitting for Positive Direction in Y-axis n = 5

From the figure (3.4), the dark blue curve is representing the fitted curve for the positive frequency readings of y-axis, from which the equation of the curve could be obtained to make the frequency curve continues instead of discrete points, so at each given point of time the frequency could be calculated. The mean of the equation is 0.38 while the standard deviation (std) is equal to 0.2193. R-square is 0.9996, equation coefficients are:

- $a_1 = 1562$
- $a_2 = 120.6$
- $a_3 = 37.51$
- $a_4 = 16.06$
- $a_5 = 33.56$
- $b_1 = 0.9033$
- $b_2 = 2.366$
- $b_3 = 7.382$
- $b_4 = 9.619$
- $b_5 = 5.332$
- $c_1 = 1.634$
- $c_2 = 2.448$
- $c_3 = -0.2469$
- $c_4 = 0.2459$
- $c_5 = 5.43$

The negative direction in figure (3.5) is the same of positive in frequency curve with different parameters values, where the mean is 0.3736, standard deviation is 0.2287, R-square is 0.9997, the following are the equation coefficients.

- $a_1 = 1564$
- $a_2 = 118.9$
- $a_3 = 36.89$
- $a_4 = 15.52$
- $a_5 = 34.37$
- $b_1 = 0.9436$
- $b_2 = 2.47$
- $b_3 = 7.755$
- $b_4 = 10.07$
- $b_5 = 5.619$
- $c_1 = -1.533$
- $c_2 = -0.7529$
- $c_3 = 2.694$
- $c_4 = 3.112$
- $c_5 = 2.147$

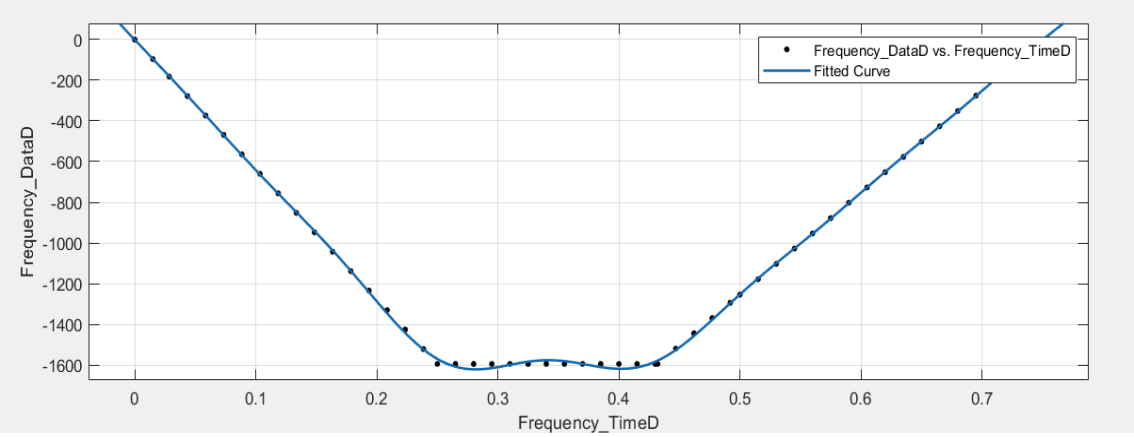

Figure3.5 Frequency Curve Fitting for Negative Direction in Y-axis n = 5

The process is the same for the position, for the same purpose, but the input of the position fitted curve will be the required moving distance, where the output will be the time interval in which the robot can travel the desired distance, where this time interval will be the input of the frequency equation (whether positive or negative direction) to obtain the frequency difference in this interval that will result is the robot moving the desired distance.

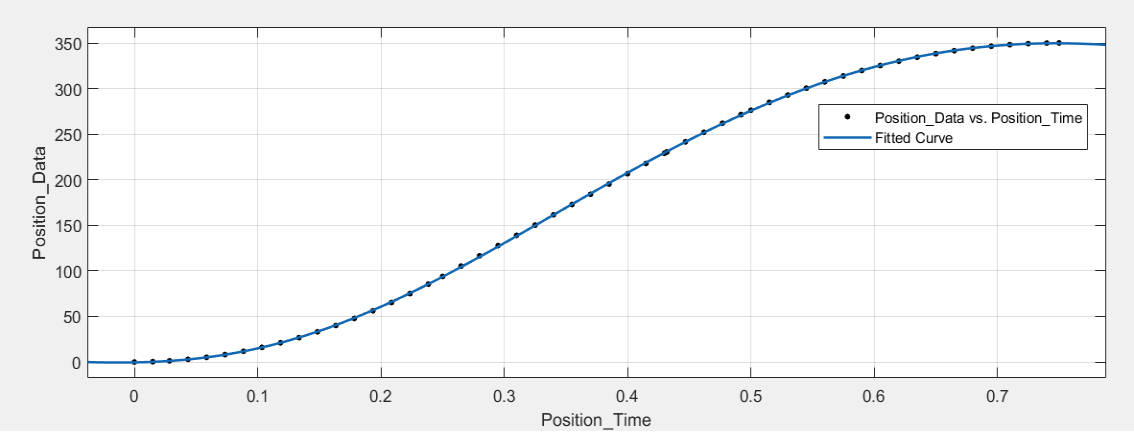

Figure3.6 Position Curve Fitting for Positive Direction in Y-axis n = 3

- $a_1 = 371.3$
- $a_2 = 68.33$
- $a_3 = 17.53$
- $Mean = 0.38$
- $b_1 = 0.2769$
- $b_2 = 1.618$
- $b_3 = 2.118$
- $std = 0.2193$
- $c_1 = 0.5502$
- $c_2 = -0.1918$
- $c_3 = 2.431$
- $R^2 = 1$

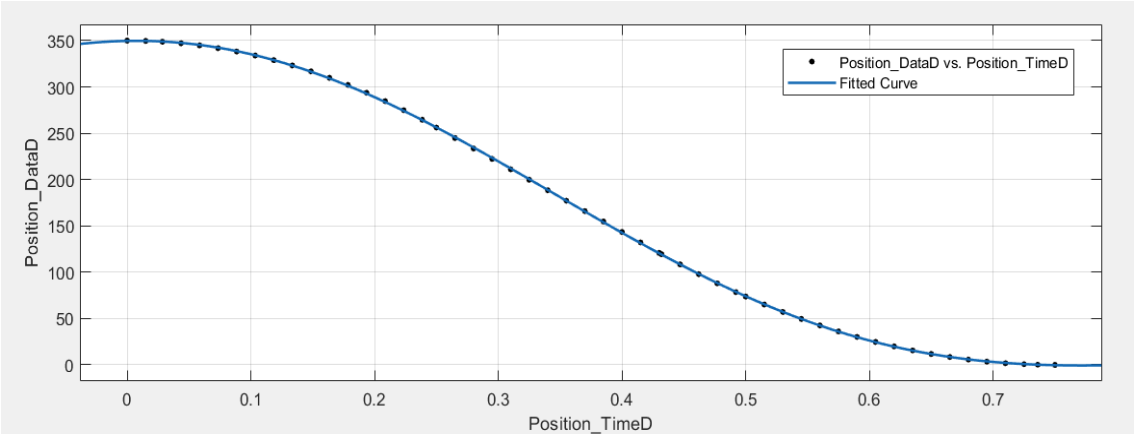

Figure3.7 Position Curve Fitting for Negative Direction in Y-axis n = 3

- $a_1 = 285.3$
- $a_2 = 80.23$
- $Mean = 0.3736$
- $b_1 = 0.343$
- $b_2 = 1.353$
- $std = 0.2287$
- $c_1 = 2.422$
- $c_2 = -2.818$
- $R^2 = 1$

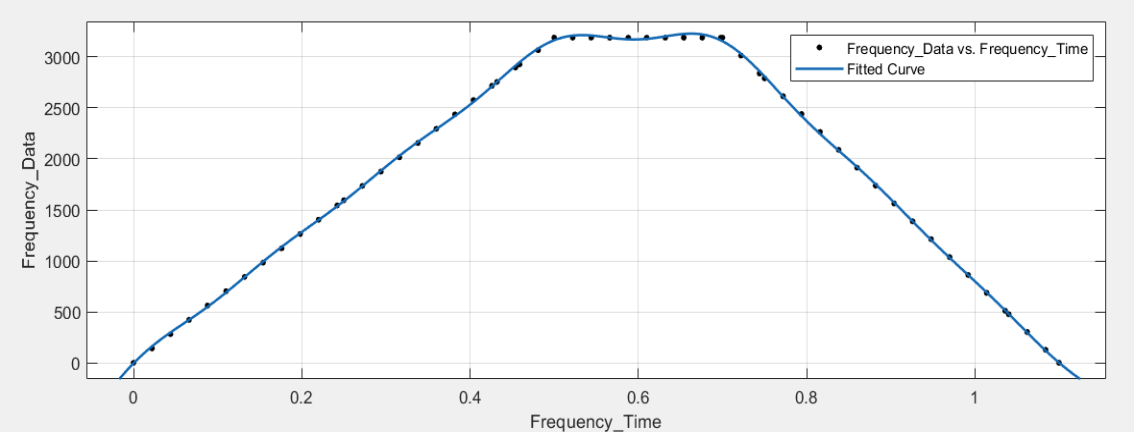

Figure3.8 Frequency Curve Fitting for Positive Direction in X-axis n = 5

- $a_1 = 3065$
- $a_2 = 30.95$
- $a_3 = 240.5$
- $a_4 = 53.75$
- $a_5 = 34.3$
- $Mean = 0.5863$
- $b_1 = 0.9499$
- $b_2 = 6.647$
- $b_3 = 2.691$
- $b_4 = 8.906$
- $b_5 = 11.63$
- $std = 0.3256$
- $c_1 = 1.49$
- $c_2 = -1.393$
- $c_3 = 1.168$
- $c_4 = -1.93$
- $c_5 = -2.065$
- $R^2 = 0.9998$

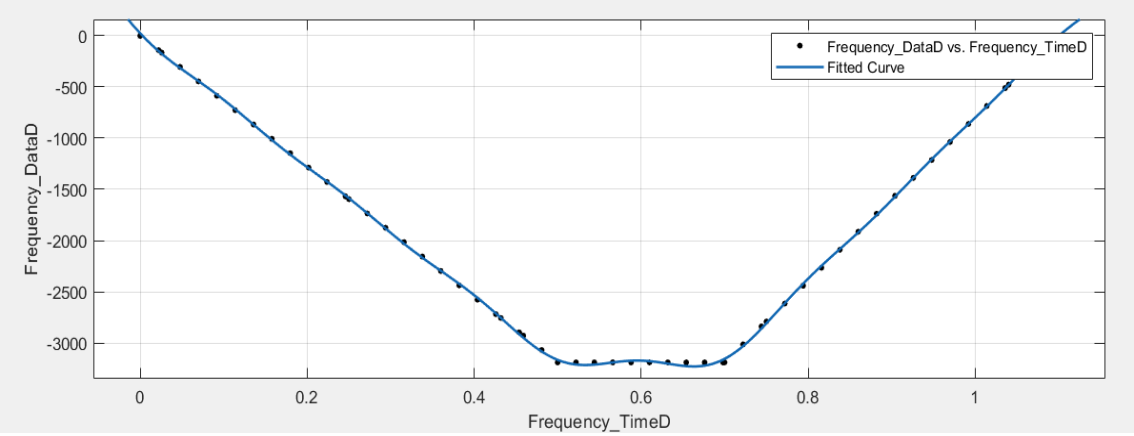

Figure3.9 Frequency Curve Fitting for Negative Direction in X-axis n = 5

- $a_1 = 3064$
- $a_2 = 29.99$
- $a_3 = 242.3$
- $a_4 = 53.88$
- $a_5 = 34.75$
- $Mean = 0.5674$
- $b_1 = 0.9741$
- $b_2 = 6.846$
- $b_3 = 3.054$
- $b_4 = 9.162$
- $b_5 = 11.98$
- $std = 0.3368$
- $c_1 = -1.586$
- $c_2 = -4.902$
- $c_3 = -2.143$
- $c_4 = 0.7026$
- $c_5 = 0.4111$
- $R^2 = 0.9998$

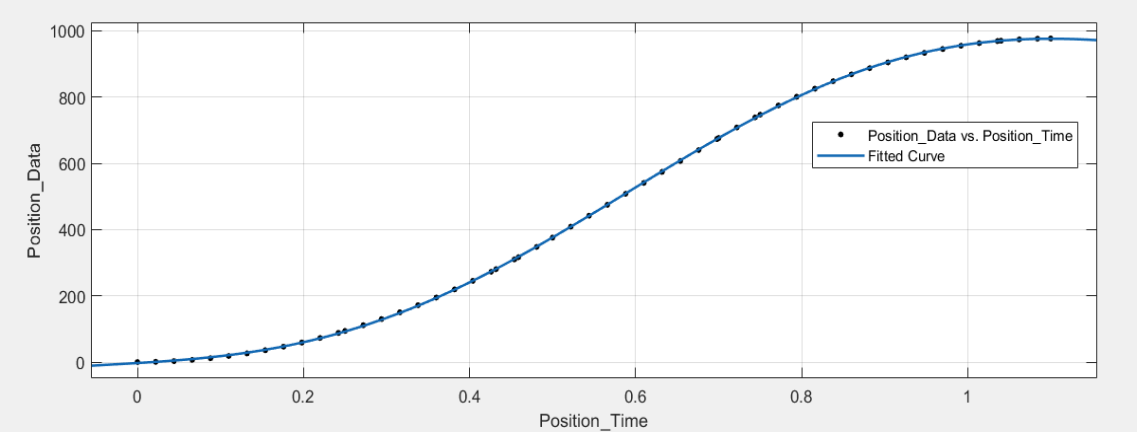

Figure3.10 Position Curve Fitting for Positive Direction in X-axis n = 2

- $a_1 = 1116$
- $b_1 = 0.26$
- $c_1 = 0.4877$
- $a_2 = 153$
- $b_2 = 1.591$
- $c_2 = -0.1102$
- $Mean = 0.5863$
- $std = 0.3256$
- $R^2 = 1$

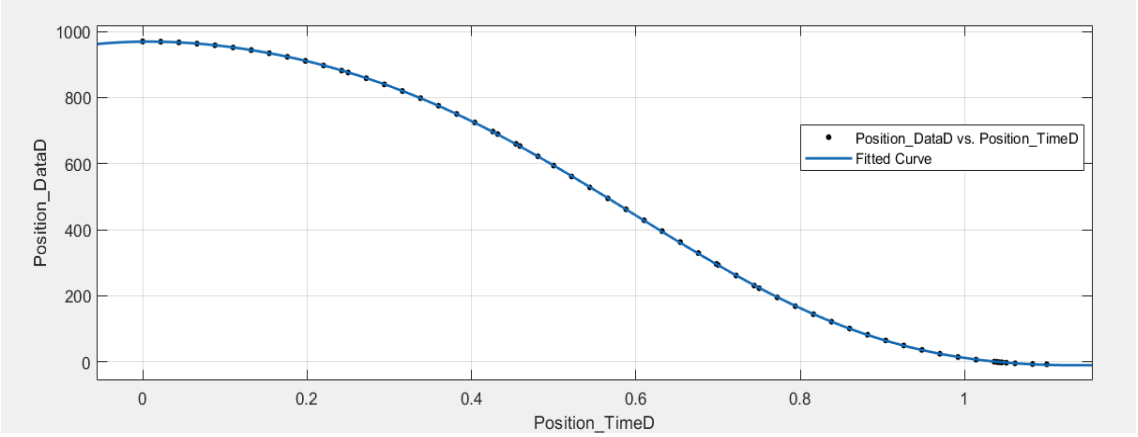

Figure3.11 Position Curve Fitting for Negative Direction in X-axis n = 3

- $a_1 = 1637$
- $b_1 = 0.604$
- $c_1 = -1.08$
- $a_2 = 1546$
- $b_2 = 0.7655$
- $c_2 = -2.473$
- $a_3 = 25.65$
- $b_3 = 2.581$
- $c_3 = 2.507$
- $Mean = 0.5674$
- $std = 0.3368$
- $R^2 = 1$

The process of motion starts with defining the required position coordinates, then substitute them in equation (3.8), and equation (3.9) to calculate the motor number of rotations needed for reaching such a position. Frequency generation is done by solving the 8 sum of sine equations, substitute for the desired position coordinate in x-axis position equation (whether positive direction or negative) to calculate the time interval in which the robot can travel such a distance. Substitute the time interval in the frequency equation (whether positive or negative direction) to calculate the frequency at each point of time that are required to move such a distance, after all apply the signal to the motor with these frequencies to reach the desired position. Same applied to the y-axis.

Chapter IV
Results and Analysis

4.1 Preface

This chapter analyze the system behavior for the inputs that is obtained in the previous chapter. In this chapter the motion of the robot will be simulated in x, and y-directions using their mathematical model, also the dynamic analysis of the mechanical structure of the system using MATLAB.

4.2 Dynamic Analysis

As a first step to simulate the model motion, mathematical model should be obtained. Mathematical model is a mathematical representation of the model in form of mathematical equations. The mathematical model is applied on systems to verify the output of the system given a certain input. According to the physical origin of the system a set of equations are used to describe it. In this project the equation of motion is used to describe the motion of the robot, where the input of the system will be the pulse rate from the motor driver, and the output will be the linear velocity of the robot, torque, position, and the acceleration. The mathematical model was made to reach the required linear velocity in accurate position with the acceleration to be controlled.

4.2.1 Mathematical Model

This section discusses how the Simulink model was built and how it was used to calculate and simulate the robot body motion in both x and y-directions. The analysis was made to simulate the real process and to attend actual and realistic results.

Robot Mathematical Model

To simulate the robot behavior a mathematical model should be done first. From equation (3.2), the mathematical model of the robot x-axis can simply be described using the following equation.

$$\boldsymbol{T = (m * \ddot{x} + 6 * m * g * \mu)\frac{d_p}{4} * S * K_a} \tag{4.1}$$

Similarly, for the y-axis. From equation (3.4), the mathematical model of the robot is described by the following.

$$\boldsymbol{T = (m * \ddot{y} + m * g) * S * K_a * \frac{d_p}{2}} \tag{4.2}$$

From the equations above the input of the system is the derivative of the velocity in each direction as the rest of the equation are constants. By knowing the linear speed of the robot, the torque required to move the robot can be calculated, the position can be estimated from integrating the speed, also the acceleration is to be obtained from the derivative of the speed. The speed is to be obtained using the motor mathematical model.

Motor Mathematical Model

To calculate the speed of the robot, a motor mathematical model should be obtained first, below is the mathematical model of the mechanical part of the motor.

$$\boldsymbol{N = \frac{Pulse\ rate}{Motor\ steps\ per\ revolution} * 60} \tag{4.3}$$

Where:

- Pulse rate = the number of driver pulses per second (pulse/sec)
- N is the motor speed (rpm)
- Motor steps/rev = number of steps the motor needs to complete a full rotation (steps/rev)

Since the motor angle for each step is 1.8˚ according to the motor datasheet, then for 360˚ the motor performs 200 steps. The pulse rate will be the input of the system, the only unknown is the motor speed. The linear velocity now can be calculated using the motor speed, where the linear velocity of the robot is described using the following equation.

$$\boldsymbol{v = \frac{N * d}{60000}} \tag{5.4}$$

From equation (3.5) d = 94.24 mm/rev, N is the motor speed in rpm that will be calculated after applying the pulse rate on the equation, thus; linear velocity is calculated and to be used in the equation of motion.

Block Diagram

The block diagram is a graphical representation of the mathematical model where the equations and the mathematical operators are replaced with functional blocks each performs a certain operation. The block diagram is done on MATLAB, so the input and output of the system are to be visualized to make the process of analysis easier.

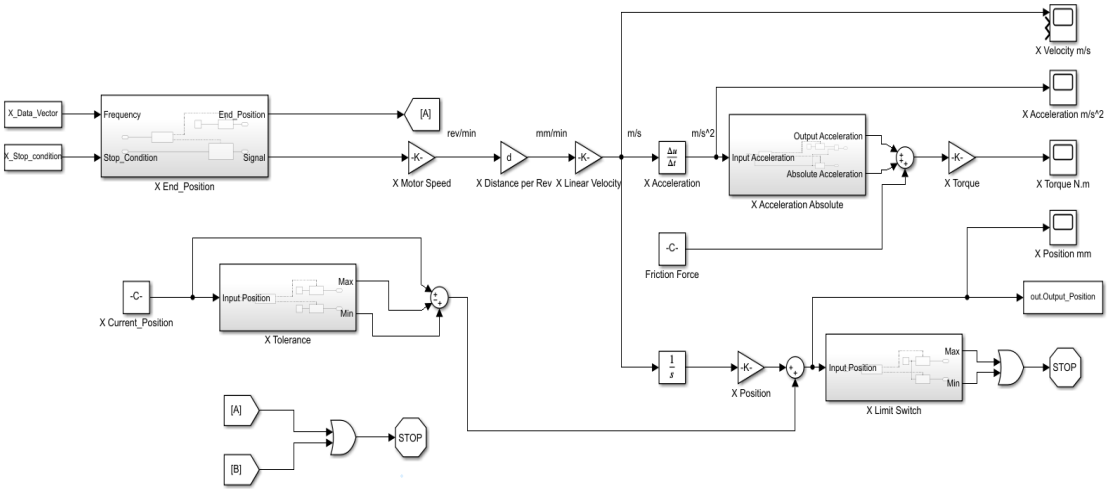

Figure4.1 X-axis Block Diagram

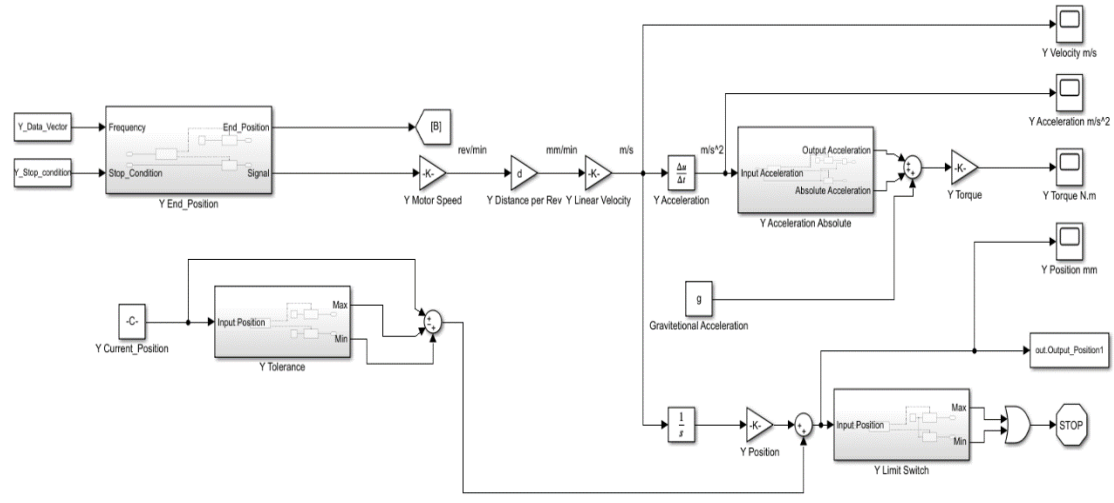

Figure 4.2 Y-axis Block Diagram

The output of these blocks is the position, the velocity and the acceleration of motion for each axis.

Dynamic Analysis

Now the system is ready for simulating the motion of the robot to reach each position where the robot must attend to pick the medicine ordered by the pharmacist. This operation is done after the robot searches for the indices of x and y coordinates and orders it to each direction's motor to reach this location. Below is a testing operation for the robot to get a medicine from the right top shelf; taking into consideration that the robot starts from left down as zero position and x is to be of 970mm and y is 340mm.

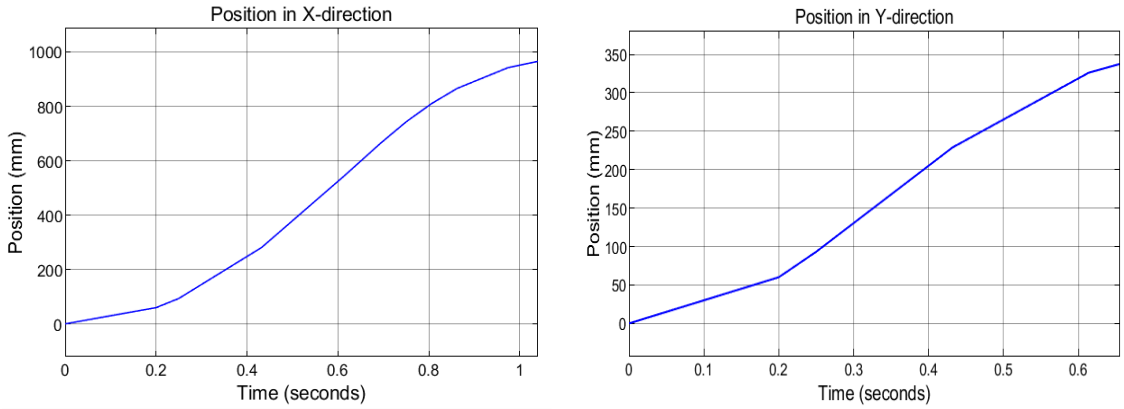

(a) (b)

Figure4.9 First Test's Position Analysis, (a) Position in X-direction and (b) Position in Y-direction

From the position curves it is observed that to reach the required position for x-direction it took the robot approximately 1.04s and for the y-direction 0.656s. Observing the rest of the requirements parameter to reach this position by their scopes to make sure that there are no undesired actions.

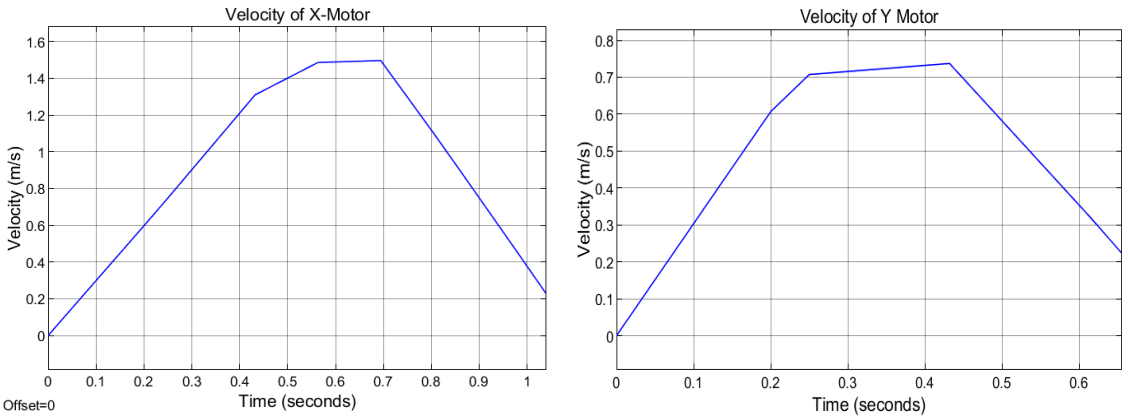

(a) (b)

Figure4.10 First Test's Velocity Analysis, (a) Velocity of X-Motor and (b) Velocity of Y-Motor

From the above curves it is observed that the velocity acts approximately in the same way, but with difference in values each with its corresponding calculated value in chapter III. The decrease in velocity is because of the robot approaches the desired position so in order to prevent that it misses the position and stop in its appropriate time as needed the robot must decelerate in a certain point that will be calculated later. Also, it is obvious that the robot reaches the position in y-direction before the one of the x-direction, so the robot stops the y-motor before the x-motor and stays at the desired location.

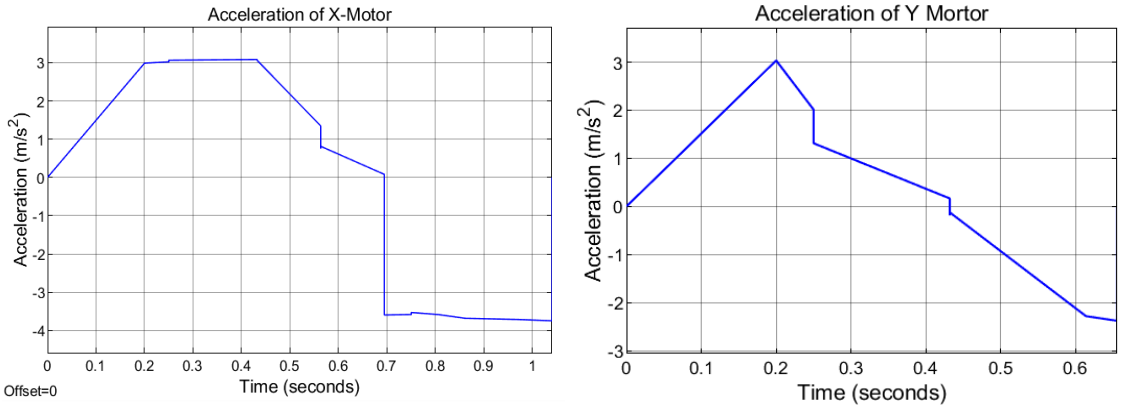

(a) (b)

Figure4.11 First Test's Acceleration Analysis, (a) Acceleration of X-Motor and (b) Acceleration of Y-Motor

Despite that the velocity decreases with approximately the same rate, the acceleration with undesired and estimated behavior. Also, it begun decelerating from the second 0.2 for the y-motor to maintain the required velocity stable and serve reaching the position accurately. The torque curve is predicted to be similar to the acceleration curve but with different values because they are directly proportional from equation (3.2) and (3.4).

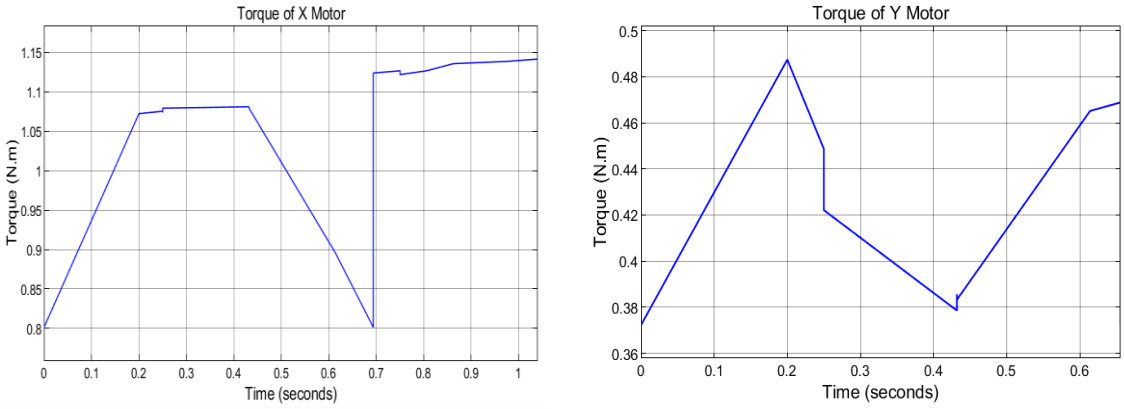

(a) (b)

Figure4.12 First Test's Torque Analysis, (a) Torque of X-Motor and (b) Torque of Y-Motor

From the previous graphs it is proved that the torque acts according to the acceleration properly which acts according to the behavior of the velocity, and due to the presence of the absolute block diagram mentioned before the torque required to speed up the operation or slowing it down is in the positive direction that is then translated to the motor to move the robot body properly.

Another test was made as there is a new request, and it was found that the required location is 500 in x-direction and 20 in y-direction; so, based on these indices a signal was sent to the motors to reach this location and get the medicine, so the analysis is as follows.

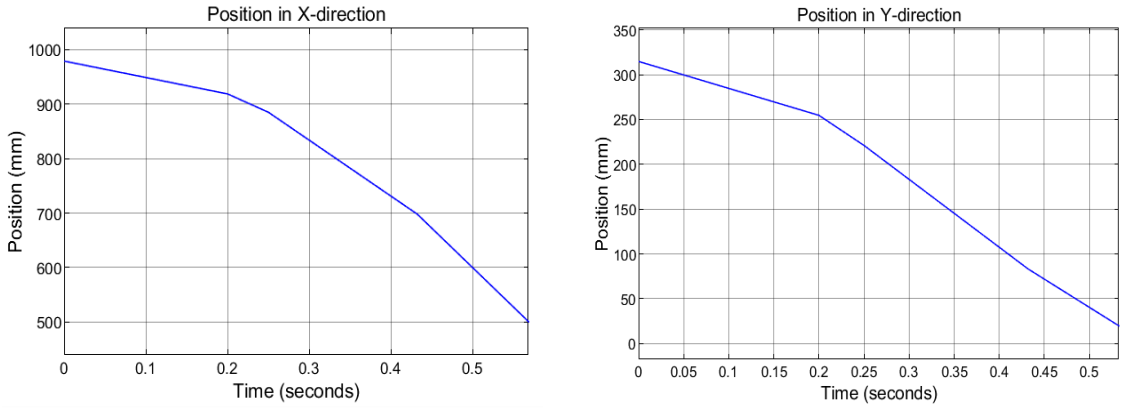

(a) (b)

Figure4.13 Second Test's Position Analysis, (a) Position in X-direction and (b) Position in Y-direction

It is observed that the model works correctly and reach the desired location as ordered; and it also satisfies the aim of the project by reaching the goal position the fastest it can as the time taken in x-direction was only 0.56s and for that in y- direction was only 0.53s so the whole operation took approximately only 0.6s.

Now to make sure that the system really simulates the real system, the velocity curves was observed in figure (5.14).

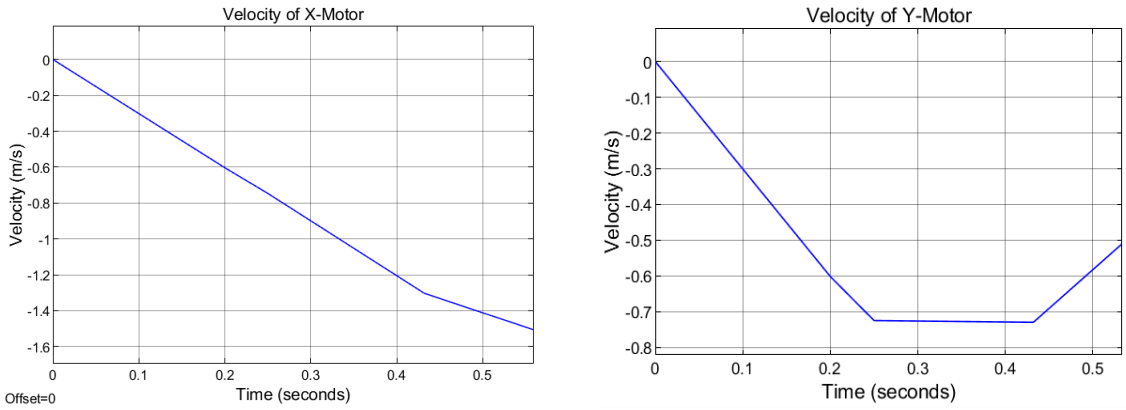

(a) (b)

Figure4.14 Second Test's Velocity Analysis, (a) Velocity of X-Motor and (b) Velocity of Y-Motor

From the above curve it is obvious that to return back to a position before the current position the robot must reach first the 0 velocity to reverse its direction and begin moving and accelerating but in the negative direction, but at some point it will reach the maximum value of the velocity due to the continuous acceleration so the negative value here indicates only the direction. Another observation from that curve is that because of the regular acceleration, the torque will act according to it also and reach the maximum torque of each motor but regularly.

The previous tests were done for a case where different drugs were ordered so they have different locations, but this is not always the case. Usually, a previous ordered medicine could be ordered another time so the test for this case is to take the same coordinates' values.

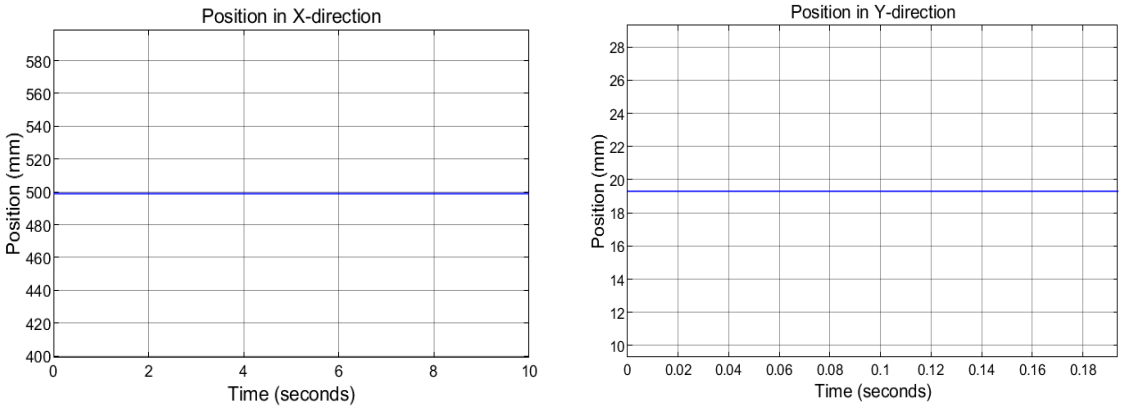

(a) (b)

Figure4.15 Third Test's Position Analysis, (a) Position in X-direction and (b) Position in Y-direction

As predicted the robot does not change its position as desired so it is obvious that there will not be any change in velocity; thus, there is no acceleration.

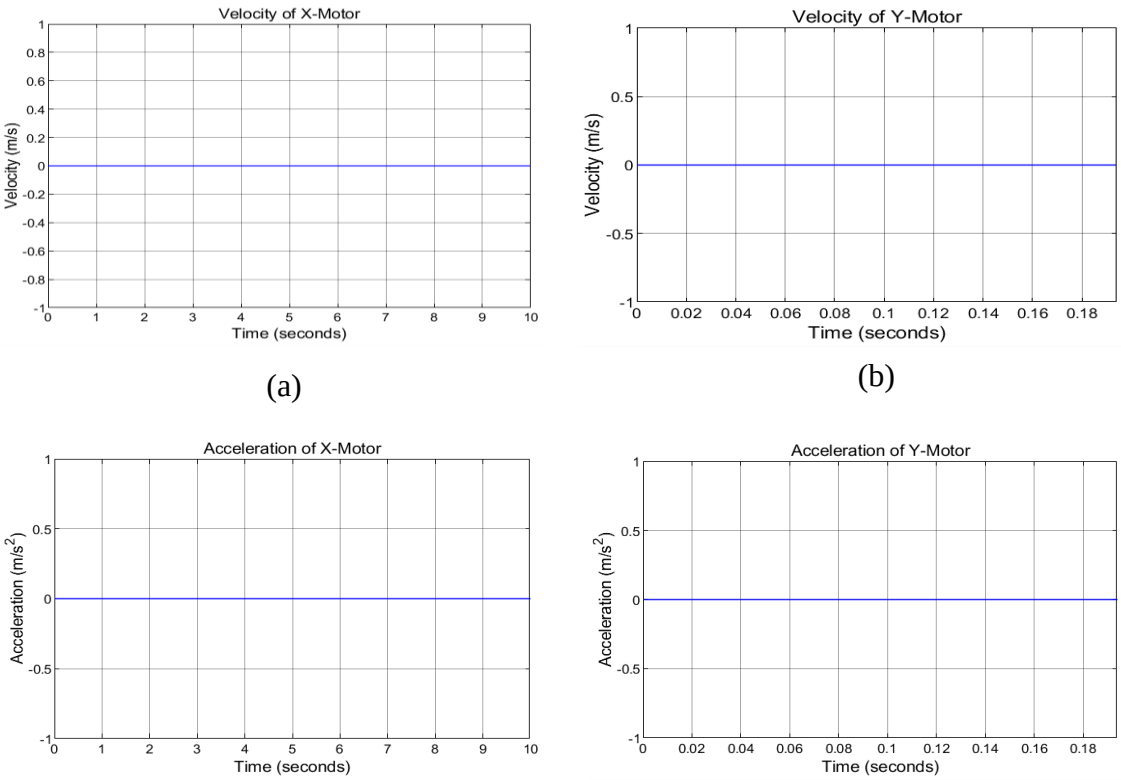

(a) (b)

(c) (d)

Figure4.16 Third Test's Analysis, (a) Velocity of X-Motor, (b) Velocity of Y-Motor, (c) Acceleration of X-Motor and (d) Acceleration of Y-Motor

The only difference was found to be in the torque curves as there is no acceleration, so the only load added to the x-direction motor was the friction force and for that of the y-direction was the weight force, so the torque does have a value but constant only to resist these loads from rotating the motor in the opposite direction, and maintain the robot static as shown in figure (5.17).

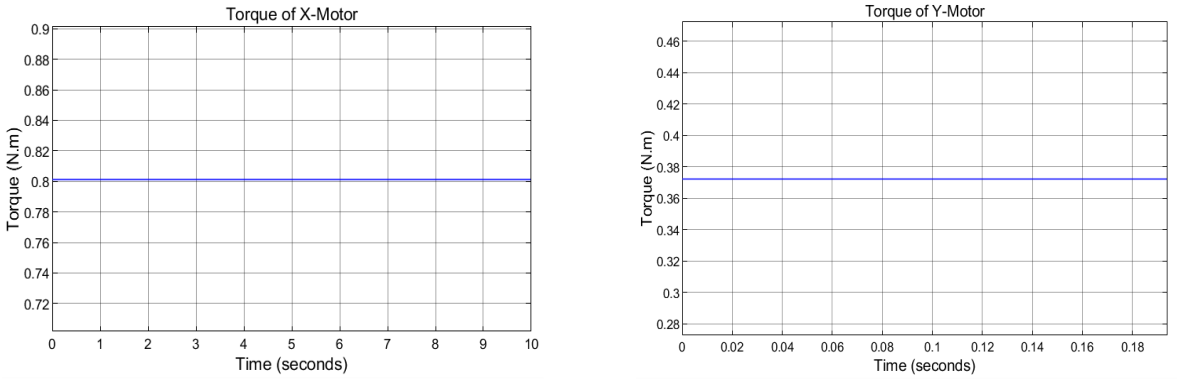

(a) (b)

Figure4.17 Third Test's Torque Analysis, (a) Torque of X-Motor and (b) Torque of Y-Motor

From all the last analysis it was obvious that the model that was made satisfies the requirements of the project with accurate positions and with the fastest response. The slowest operation may take only 1.04s where it is traveling the maximum distance it could be. So, the only need for reaching any additional position is to detect its coordinates and the robot behavior might be as one of the three cases illustrated in this section.

Chapter V
Conclusions and Future Work

5.1 Conclusions

The project aim is the design and implementation of an automated channel-fed drug dispensing system to help in making the process of drug dispensing easier, faster, and more precise. Consequently, the following objectives were fulfilled:

- A literature survey was conducted in the field of automated drug dispensing systems.
- A suitable design is selected based on the literature survey.
- A Cartesian robot for 2D motion was designed.
- A suitable shelf that can serve the operation was designed.
- System components were analyzed.
- System was modeled and simulated MATLAB.

5.2 Future Work

To reach our aim of the designing and implementing an automated channel-fed drug dispensing system, the following will be executed:

- Develop a searching algorithm to make the process of dispensing faster.
- Improve the capacity efficiency of such a system.
- Improve the safety of the dispensing.
- Implement the system.
- Test the system functionality.
- Publish a paper on such a new field.

References

Chole, K. (2021) ‘Drug dispensing goes digital’, *Pharmaceutical technology*. Available at: https://www.pharmaceutical-technology.com/analysis/robotic-drug-dispensing-digital-pharmacy/

Dhaware, Y. *et al.* (2008) ‘Review on Comparative Analysis of Ball Screw & Lead Screw’, *International Research Journal of Engineering and Technology*, p. 769. Available at: www.irjet.net.

Domek, G., Krawiec, P. and Wilczyński, M. (2018) ‘Timing belt in power transmission and conveying system’, in *MATEC Web of Conferences*. EDP Sciences. Available at: https://doi.org/10.1051/matecconf/201815704001.

Ehrmann, C., Isabey, P. and Fleischer, J. (2016) ‘Condition Monitoring of Rack and Pinion Drive Systems: Necessity and Challenges in Production Environments’, in *Procedia CIRP*. Elsevier B.V., pp. 197–201. Available at: https://doi.org/10.1016/j.procir.2016.01.101.

Fenercioğlu, A. *et al.* (2011) *Automatic Storage and Retrieval System (AS/RS) Based on Cartesian Robot for Liquid Food Industry TRAJECTORY DETERMINATION, OPTIMIZATION OF KINEMATICS AND SIMULATION OF CUTTER ON CNC CAMSHAFT GRINDING PROCESS View Project Eddy current separator design View project*. Available at: https://www.researchgate.net/publication/292762869.

Gonnet, G.H., Rogers, L.D. and George, J.A. (1980) *An Algorithmic and Complexity Analysis of Interpolation Search, Acta Informatica*.

Hachemi Université D’oran, K. and Ahmed, M. ben (2014) *Design of a control and tracking framework of an automated drug dispensing system Performance evaluation of Drug dispensing systems View project*. Available at: https://www.researchgate.net/publication/309677651.

Hajdučík, A., Škrabala, J. and Medvecky, S. (2019) *Conceptual design of a drug dispenser Optimum preload for rolling bearings View project high temperature furnace for crystal growth View project*. Available at : https://www.researchgate.net/publication/332320383.

Hoda, M.N. *et al.* (*2015*) *International Conference on Computing for Sustainable Global Development (INDIACom): 11th to 13th March, 2015, Bharati Vidyapeeth’s Institute of Computers, Applications and Management (BVICAM)*.

Karthikeyan M (2015) ‘A Systematic Review on Medication Errors Isolation of anti-inflammatory agents from medicinal plants View project Bentham Brand Ambassador for Bentham Science Publishers View Project International Journal of Drug Development and Research’, *Int J Drug Dev & Res*, 7(4), p. 4. Available at: https://www.researchgate.net/publication/289527058.

Mehmood, A. (2019) ‘ASH Search: Binary Search Optimization’, *International Journal of Computer Applications*, 178(15), pp. 10–17. Available at : https://doi.org/10.5120/ijca2019918788.

Mehta, A. *et al.* (2015) ‘Impact Factor (PIF): 2.243 International Journal OF Engineering Sciences & Management Research A REVIEW ON COMPARISION OF BINARY SEARCH

AND LINEAR SEARCH', *International Journal of Engineering Sciences & Management Research*, 2(10). Available at : http://www.ijesmr.com©.

Morrison, D. *et al.* (2018) 'Cartman: The Low-Cost Cartesian Manipulator that Won the Amazon Robotics Challenge', in *Proceedings - IEEE International Conference on Robotics and Automation*. Institute of Electrical and Electronics Engineers Inc., pp. 7757–7764. Available at: https://doi.org/10.1109/ICRA.2018.8463191.

Mu'min, *et al.* (2017) *Automated Drugs Dispenser Machine (ADM)*.

Shawn, C. and Pulle, S. (2014) *Design and Control of a 3-Axis Articulated Pick and Place Robot*.

Stojanovic, B., Marjanovic, N. and Blagojevic, M. (2011) *Failure analysis of the timing belt drives Application of Taguchi method View project Cycloidal Speed Reducer View project*. Available at: https://www.researchgate.net/publication/271705831.

Thanaboonkong, K. and Suthakorn, J. (2014) 'A study and development on robotic drug storaging and dispensing system in drug logistics for a mid-sized hospital', in *2014 IEEE International Conference on Robotics and Biomimetics, IEEE ROBIO 2014*. Institute of Electrical and Electronics Engineers Inc., pp. 2116–2120. Available at: https://doi.org/10.1109/ROBIO.2014.7090649.